chapter**THIRTEEN**

An Introduction to Ultraviolet-Visible Molecular Absorption Spectrometry

Molecular absorption spectroscopy in the ultraviolet and visible spectral regions is widely used for the quantitative determination of a large number of inorganic, organic, and biological species. In this chapter, we introduce the principles of molecular absorption spectroscopy based on electromagnetic radiation in the wavelength region of 190 to 800 nm. Many of these principles, however, are applicable to spectroscopic measurements in other spectral regions such as the infrared region.

Throughout this chapter, this logo indicates an opportunity for online self-study at **www.tinyurl.com/skoogpia7**, linking you to interactive tutorials, simulations, and exercises.

Molecular absorption spectroscopy[1] is based on the measurement of the transmittance T or the absorbance A of solutions contained in transparent cells having a path length of b centimeters. Ordinarily, the concentration of an absorbing analyte is linearly related to absorbance as given by Beer's law:

$$A = -\log T = \log \frac{P_0}{P} = \varepsilon bc \qquad (13\text{-}1)$$

All of the variables in this equation are defined in Table 13-1.

13A MEASUREMENT OF TRANSMITTANCE AND ABSORBANCE

Transmittance and absorbance, as defined in Table 13-1, cannot normally be measured in the laboratory because the analyte solution must be held in a transparent container, or cell. As shown in Figure 13-1, reflection occurs at the two air-wall interfaces as well as at the two wall-solution interfaces. The resulting beam attenuation is substantial, as we demonstrated in Example 6-2, where it was shown that about 8.5% of a beam of yellow light is lost by reflection in passing through a glass cell containing water. In addition, attenuation of a beam may occur as a result of scattering by large molecules and sometimes from absorption by the container walls. To compensate for these effects, the power of the beam transmitted by the analyte solution is usually compared with the power of the beam transmitted by an identical cell containing only solvent. An experimental transmittance and absorbance that closely approximate the true transmittance and absorbance are then obtained with the equations

$$T = \frac{P_{\text{solution}}}{P_{\text{solvent}}} \approx \frac{P}{P_0} \qquad (13\text{-}2)$$

$$A = \log \frac{P_{\text{solvent}}}{P_{\text{solution}}} \approx \log \frac{P_0}{P} \qquad (13\text{-}3)$$

[1]For further study, see F. Settle, ed., *Handbook of Instrumental Techniques for Analytical Chemistry*, Upper Saddle River, NJ: Prentice-Hall, 1997, Sections III and IV; J. D. Ingle Jr. and S. R. Crouch, *Spectrochemical Analysis*, Upper Saddle River, NJ: Prentice Hall, 1988; E. J. Meehan, in *Treatise on Analytical Chemistry*, 2nd ed., Part I, Vol. 7, Chaps. 1–3, P. J. Elving, E. J. Meehan, and I. M. Kolthoff, eds., New York, NY: Wiley, 1981; J. E. Crooks, *The Spectrum in Chemistry*, New York: Academic Press, 1978.

TABLE 13-1 Important Terms and Symbols for Absorption Measurements

Term and Symbol*	Definition	Alternative Name and Symbol
Incident radiant power, P_0	Radiant power in watts incident on sample	Incident intensity, I_0
Transmitted radiant power, P	Radiant power transmitted by sample	Transmitted intensity, I
Absorbance, A	$\log(P_0/P)$	Optical density, D; extinction, E
Transmittance, T	P/P_0	Transmission, T
Path length of sample, b	Length over which attenuation occurs	l, d
Concentration of absorber, c	Concentration in specified units	
Absorptivity,† a	$A/(bc)$	Extinction coefficient, k
Molar absorptivity,‡ ε	$A/(bc)$	Molar extinction coefficient

*Terminology recommended by the American Chemical Society (*Anal. Chem.*, **1990**, *62*, 91).

†c may be expressed in grams per liter or in other specified concentration units; b may be expressed in centimeters or other units of length.

‡c is expressed in moles per liter; b is expressed in centimeters.

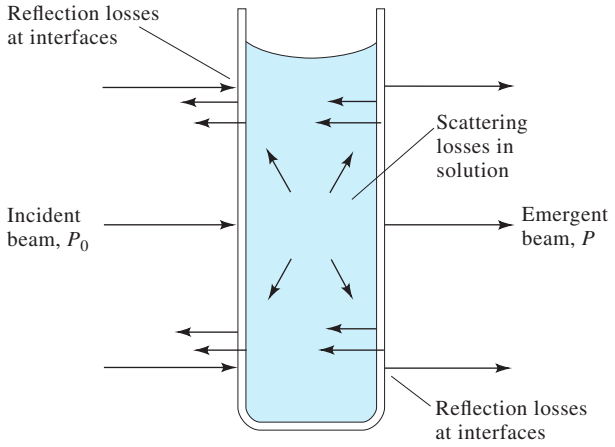

FIGURE 13-1 Reflection and scattering losses with a solution contained in a typical glass cell. Losses by reflection can occur at all the boundaries that separate the different materials. In this example, the light passes through the air-glass, glass-solution, solution-glass, and glass-air interfaces.

The terms P_0 and P, as used in the remainder of this book, refer to the power of radiation after it has passed through cells containing the solvent and the analyte solutions, respectively.

13B BEER'S LAW

Equation 13-1 represents Beer's law. This relationship can be rationalized as follows.[2] Consider the block of absorbing matter (solid, liquid, or gas) shown in Figure 13-2. A beam of parallel monochromatic radiation with power P_0 strikes the block perpendicular to a surface. After passing through a length b of the

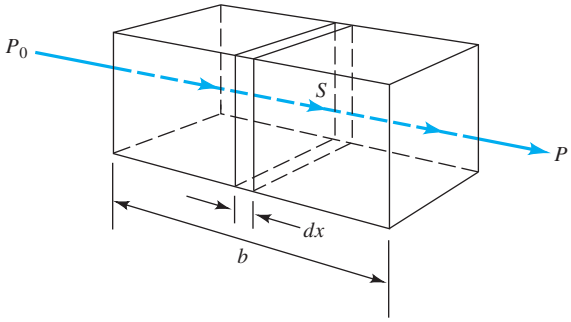

FIGURE 13-2 Radiation of initial radiant power P_0 is attenuated to transmitted power P by a solution containing c moles per liter of absorbing solution with a path length of b centimeters.

material, which contains n absorbing atoms, ions, or molecules, its power is decreased to P as a result of absorption. Consider now a cross section of the block having an area S and an infinitesimal thickness dx. Within this section there are dn absorbing particles; we can imagine a surface associated with each particle at which photon capture will occur. That is, if a photon reaches one of these areas by chance, absorption will follow immediately. The total projected area of these capture surfaces within the section is designated as dS; the ratio of the capture area to the total area, then, is dS/S. On a statistical average, this ratio represents the probability for the capture of photons within the section.

The power of the beam entering the section, P_x, is proportional to the number of photons per unit area, and dP_x represents the power absorbed within the section. The fraction absorbed is then $-dP_x/P_x$, and this ratio also equals the average probability for capture. The term is given a minus sign to indicate that the radiant power P decreases as it passes through the absorbing region. Thus,

$$-\frac{dP_x}{P_x} = \frac{dS}{S} \tag{13-4}$$

[2]The discussion that follows is based on a paper by F. C. Strong, *Anal. Chem.*, **1952**, *24*, 338, **DOI**: 10.1021/ac60062a020.

Recall, now, that dS is the sum of the capture areas for particles within the section; it must therefore be proportional to the number of particles, or

$$dS = a\,dn \tag{13-5}$$

where dn is the number of particles and a is a proportionality constant, which can be called the *capture cross section*. Combining Equations 13-4 and 13-5 and integrating over the interval between 0 and n, we obtain

$$-\int_{P_0}^{P}\frac{dP_x}{P_x} = \int_0^n \frac{a\,dn}{S}$$

When these integrals are evaluated, we find that

$$-\ln\frac{P}{P_0} = \frac{an}{S}$$

After converting to base 10 logarithms and inverting the fraction to change the sign, we obtain

$$\log\frac{P_0}{P} = \frac{an}{2.303S} \tag{13-6}$$

where n is the total number of particles within the block shown in Figure 13-2. The cross-sectional area S can be expressed as the ratio of the volume of the block V in cubic centimeters to its length b in centimeters. Thus,

$$S = \frac{V}{b}\,\text{cm}^2$$

Substitution of this quantity into Equation 13-6 yields

$$\log\frac{P_0}{P} = \frac{anb}{2.303V} \tag{13-7}$$

Note that n/V is the number of particles per cubic centimeter, which has the units of concentration. We can then convert n/V to moles per liter because the number of moles is given by

$$\text{number mol} = \frac{n\ \text{particles}}{6.02\times10^{23}\ \text{particles/mol}}$$

and c in moles per liter is given by

$$c = \frac{n}{6.02\times10^{23}}\,\text{mol}\times\frac{1000\ \text{cm}^3/\text{L}}{V\ \text{cm}^3}$$

$$= \frac{1000n}{6.02\times10^{23}V}\,\text{mol/L}$$

Combining this relationship with Equation 13-7 yields

$$\log\frac{P_0}{P} = \frac{6.02\times10^{23}abc}{2.303\times1000}$$

Finally, the constants in this equation can be collected into a single term ε to give

$$\log\frac{P_0}{P} = \varepsilon bc = A \tag{13-8}$$

which is Beer's law.

13B-1 Application of Beer's Law to Mixtures

Beer's law also applies to a medium containing more than one kind of absorbing substance. Provided that the species do not interact, the total absorbance for a multicomponent system is given by

$$A_{\text{total}} = A_1 + A_2 + \cdots + A_n$$

$$= \varepsilon_1 bc_1 + \varepsilon_2 bc_2 + \cdots + \varepsilon_n bc_n \tag{13-9}$$

where the subscripts refer to absorbing components 1, 2, . . . , n.

13B-2 Limitations to Beer's Law

Few exceptions are found to the generalization that absorbance is linearly related to path length. On the other hand, deviations from the direct proportionality between the measured absorbance and concentration frequently occur when b is constant. Some of these deviations, called *real deviations*, are fundamental and represent real limitations of the law. Others are a result of how the absorbance measurements are made (*instrumental deviations*) or a result of chemical changes that occur when the concentration changes (*chemical deviations*).

Real Limitations to Beer's Law

Beer's law describes the absorption behavior of media containing relatively low analyte concentrations; in this sense, it is a limiting law. At high concentrations (usually >0.01 M), the extent of solute-solvent interactions, solute-solute interactions, or hydrogen bonding can affect the analyte environment and its absorptivity. For example, at high concentrations, the average distances between the molecules or ions responsible for absorption are diminished to the point where each particle affects the charge distribution of its neighbors. These solute-solute interactions can alter the ability of the analyte species to absorb a given wavelength of radiation. Because the extent of interaction depends on concentration, deviations from the linear relationship between absorbance and concentration occur. A similar effect is sometimes encountered in media containing low absorber concentrations but high concentrations of other species, particularly electrolytes. The proximity of ions to the absorber alters the molar absorptivity of the latter by electrostatic interactions; the effect is lessened by dilution.

Although the effect of molecular interactions is ordinarily not significant at concentrations below 0.01 M, some exceptions occur among certain large organic ions or molecules. For example, the molar absorptivity at 436 nm for the cation of methylene blue in aqueous solutions is reported to increase by 88% as the dye concentration is increased from 10^{-5} to 10^{-2} M; even below 10^{-6} M, strict adherence to Beer's law is not observed.

Exercise: Learn more about **absorption spectrophotometry** at www.tinyurl.com/skoogpia7

Deviations from Beer's law also arise because absorptivity depends on the refractive index of the medium.[3] Thus, if concentration changes cause significant alterations in the refractive index n of a solution, departures from Beer's law are observed. A correction for this effect can be made by substituting the quantity $\varepsilon n/(n^2 + 2)^2$ for ε in Equation 13-8. In general, this correction is never very large and is rarely significant at concentrations less than 0.01 M.

Apparent Chemical Deviations

Apparent deviations from Beer's law arise when an analyte dissociates, associates, or reacts with a solvent to produce a product with different absorption characteristics than the analyte. A common example of this behavior is found with aqueous solutions of acid-base indicators. For example, the color change associated with a typical indicator HIn arises from shifts in the equilibrium

$$\underset{\text{color 1}}{\text{HIn}} \rightleftharpoons \text{H}^+ + \underset{\text{color 2}}{\text{In}^-}$$

Example 13-1 demonstrates how the shift in this equilibrium with dilution results in deviation from Beer's law.

EXAMPLE 13-1

Solutions containing various concentrations of the acidic indicator HIn with $K_a = 1.42 \times 10^{-5}$ were prepared in 0.1 M HCl and 0.1 M NaOH. In both media, plots of absorbance at either 430 nm or 570 nm versus the total indicator concentration are nonlinear. However, in both media, Beer's law is obeyed at 430 nm and 570 nm for the individual species HIn and In^-. Hence, if we knew the equilibrium concentrations of HIn and In^-, we could compensate for the dissociation of HIn. Usually, though, the individual concentrations are unknown and only the total concentration $c_{total} = [HIn] + [In^-]$ is known.

We now calculate the absorbance for a solution with $c_{total} = 2.00 \times 10^{-5}$ M. The magnitude of the acid dissociation constant suggests that, for all practical purposes, the indicator is entirely in the undissociated HIn form in the HCl solution and completely dissociated as In^- in NaOH. The molar absorptivities at 430 and 570 nm of the weak acid HIn and its conjugate base In^- were determined by measurements of strongly acidic and strongly basic solutions of the indicator. The results were

	ε_{430}	ε_{570}
HIn	6.30×10^2	7.12×10^3
In^-	2.06×10^4	9.61×10^2

What are the absorbances (1.00-cm cell) of unbuffered solutions of the indicator ranging in concentration from 2.00×10^{-5} M to 16.00×10^{-5} M?

Solution

First, we find the concentration of HIn and In^- in the unbuffered 2×10^{-5} M solution. Here,

$$\text{HIn} \rightleftharpoons \text{H}^+ + \text{In}^-$$

and

$$K_a = 1.42 \times 10^{-5} = \frac{[\text{H}^+][\text{In}^-]}{[\text{HIn}]}$$

From the equation for the dissociation reaction, we know that $[H^+] = [In^-]$. Furthermore, the mass balance expression for the indicator tells us that $[In^-] + [HIn] = 2.00 \times 10^{-5}$ M. Substitution of these relationships into the K_a expression yields

$$\frac{[\text{In}^-]^2}{2.00 \times 10^{-5} - [\text{In}^-]} = 1.42 \times 10^{-5}$$

Rearrangement yields the quadratic expression

$$[\text{In}^-]^2 + (1.42 \times 10^{-5}[\text{In}^-]) - (2.84 \times 10^{-10}) = 0$$

The positive solution to this equation is

$$[\text{In}^-] = 1.12 \times 10^{-5}\ \text{M}$$

and

$$\begin{aligned}[\text{HIn}] &= (2.00 \times 10^{-5}) - (1.12 \times 10^{-5}) \\ &= 0.88 \times 10^{-5}\ \text{M}\end{aligned}$$

We are now able to calculate the absorbance at the two wavelengths. For 430 nm, we can substitute into Equation 13-9 and obtain

$$\begin{aligned}A &= \varepsilon_{\text{In}^-} b[\text{In}^-] + \varepsilon_{\text{HIn}} b[\text{HIn}] \\ A_{430} &= (2.06 \times 10^4 \times 1.00 \times 1.12 \times 10^{-5}) \\ &\quad + (6.30 \times 10^2 \times 1.00 \times 0.88 \times 10^{-5}) \\ &= 0.236\end{aligned}$$

Similarly at 570 nm,

$$\begin{aligned}A_{570} &= (9.61 \times 10^2 \times 1.00 \times 1.12 \times 10^{-5}) \\ &\quad + (7.12 \times 10^3 \times 1.00 \times 0.88 \times 10^{-5}) \\ &= 0.073\end{aligned}$$

Additional data, obtained in the same way, are shown in Table 13-2.

The plots in Figure 13-3, which contain the data from Table 13-2, illustrate the types of departures from Beer's law that occur when the absorbing system undergoes dissociation or association. Note that the direction of curvature is opposite at the two wavelengths.

[3] G. Kortum and M. Seiler, *Angew. Chem.*, **1939**, *52*, 687; **DOI**: 10.1002/ange.19390524802.

TABLE 13-2 Calculated Absorbance Data for Various Indicator Concentrations

c_{HIn}, M	[HIn], M	[In^-], M	A_{430}	A_{570}
2.00×10^{-5}	0.88×10^{-5}	1.12×10^{-5}	0.236	0.073
4.00×10^{-5}	2.22×10^{-5}	1.78×10^{-5}	0.381	0.175
8.00×10^{-5}	5.27×10^{-5}	2.73×10^{-5}	0.596	0.401
12.0×10^{-5}	8.52×10^{-5}	3.48×10^{-5}	0.771	0.640
16.0×10^{-5}	11.9×10^{-5}	4.11×10^{-5}	0.922	0.887

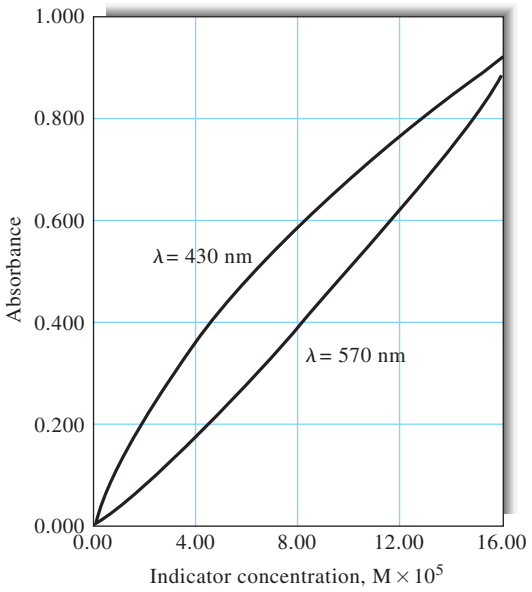

FIGURE 13-3 Chemical deviations from Beer's law for unbuffered solutions of the indicator HIn. For the data, see Example 13-1. Note that there are positive deviations at 430 nm and negative deviations at 570 nm. At 430 nm, the absorbance is primarily due to the ionized In^- form of the indicator and is proportional to the fraction ionized, which varies nonlinearly with the total indicator concentration. At 570 nm, the absorbance is due principally to the undissociated acid HIn, which increases nonlinearly with the total concentration.

Instrumental Deviations due to Polychromatic Radiation

Beer's law strictly applies only when measurements are made with monochromatic source radiation. In practice, polychromatic sources that have a continuous distribution of wavelengths are used in conjunction with a grating or with a filter to isolate a nearly symmetric band of wavelengths surrounding the wavelength to be used (see Figures 7-13, 7-16, and 7-17, for example).

The following derivation shows the effect of polychromatic radiation on Beer's law. Consider a beam of radiation consisting of just two wavelengths λ' and λ''. Assuming that Beer's law applies strictly for each wavelength, we may write for λ'

$$A' = \log\frac{P_0'}{P'} = \varepsilon' bc$$

or

$$\frac{P_0'}{P'} = 10^{\varepsilon' bc}$$

and

$$P' = P_0' 10^{-\varepsilon' bc}$$

Similarly, for the second wavelength λ''

$$P'' = P_0'' 10^{-\varepsilon'' bc}$$

When an absorbance measurement is made with radiation composed of both wavelengths, the power of the beam emerging from the solution is the sum of the powers emerging at the two wavelengths, $P' + P''$. Likewise, the total incident power is the sum $P_0' + P_0''$. Therefore, the measured absorbance A_m is

$$A_m = \log\frac{(P_0' + P_0'')}{(P' + P'')}$$

We then substitute for P' and P'' and find that

$$A_m = \log\frac{(P_0' + P_0'')}{(P_0' 10^{-\varepsilon' bc} + P_0'' 10^{-\varepsilon'' bc})}$$

When the molar absorptivities are the same at the two wavelengths ($\varepsilon' = \varepsilon''$), this equation simplifies to

$$A_m = \varepsilon' bc = \varepsilon'' bc$$

and Beer's law is followed. As shown in Figure 13-4, however, the relationship between A_m and concentration is no longer linear when the molar absorptivities differ. In addition, as the difference between ε' and ε'' increases, the deviation from linearity increases. The same effect is observed when additional wavelengths are included.

If the band of wavelengths selected for spectrophotometric measurements corresponds to a region of the absorption spectrum in which the molar absorptivity of the analyte is essentially constant, departures from Beer's law are minimal. Many molecular bands in the ultraviolet (UV)-visible region fit this description. For these, Beer's law is obeyed as demonstrated by Band *A* in Figure 13-5. On the other hand, some absorption bands in the UV-visible region and many in the infrared (IR) region are very narrow, and departures from Beer's law are common, as illustrated for Band *B* in Figure 13-5. Hence, to avoid

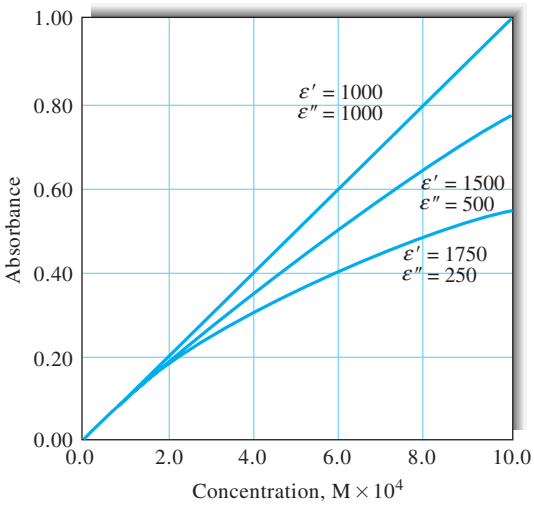

FIGURE 13-4 Deviations from Beer's law with polychromatic radiation. The absorber has the indicated molar absorptivities at the two wavelengths λ' and λ''.

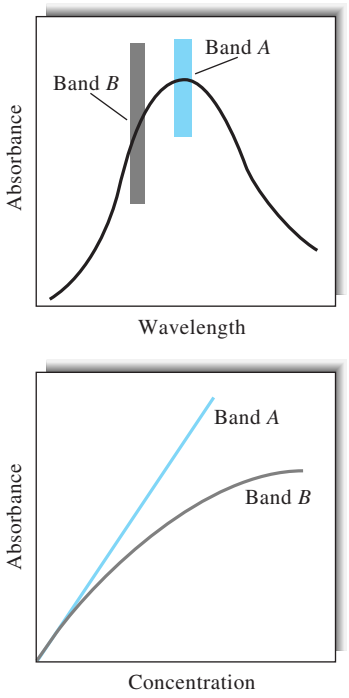

FIGURE 13-5 The effect of polychromatic radiation on Beer's law. In the spectrum at the top, the absorptivity of the analyte is nearly constant over Band *A* from the source. Note in the Beer's law plot at the bottom that using Band *A* gives a linear relationship. In the spectrum, Band *B* corresponds to a region where the absorptivity shows substantial changes. In the lower plot, note the dramatic deviation from Beer's law that results.

deviations, it is advisable to select a wavelength band near the wavelength of maximum absorption where the analyte absorptivity changes little with wavelength.

It is also found experimentally that for absorbance measurements at the maximum of narrow bands, departures from Beer's law are not significant if the effective bandwidth of the monochromator or filter $\Delta\lambda_{eff}$ (Equation 7-17) is less than one tenth of the width of the absorption band at half height (full width at half maximum).

Instrumental Deviations in the Presence of Stray Radiation

We showed in Chapter 7 that the radiation exiting from a monochromator is usually contaminated with small amounts of scattered or stray radiation. This radiation, commonly called *stray light*, is defined as radiation from the instrument that is outside the nominal wavelength band chosen for the determination. This stray radiation often is the result of scattering and reflection off the surfaces of gratings, lenses or mirrors, filters, and windows. The wavelength of stray radiation often differs greatly from that of the principal radiation and, in addition, the radiation may not have passed through the sample.

When measurements are made in the presence of stray radiation, the observed absorbance A' is given by

$$A' = \log \frac{P_0 + P_s}{P + P_s}$$

where P_s is the power of nonabsorbed stray radiation. Figure 13-6 shows a plot of A' versus concentration for various ratios of P_s to P_0. Note that at high concentrations and at longer path lengths stray radiation can also cause significant deviations from the linear relationship between absorbance and path length.[4]

Note also that the instrumental deviations illustrated in Figures 13-5 and 13-6 result in absorbances that are smaller than theoretical. It can be shown that instrumental deviations always lead to negative absorbance errors.[5]

Mismatched Cells

Another almost trivial, but important, deviation from adherence to Beer's law is caused by mismatched cells. If the cells holding the analyte and blank solutions are not of equal path length and equivalent in optical characteristics, an intercept k will occur in the calibration curve and $A = \varepsilon bc + k$ will be the actual equation instead of Equation 13-1. This error can be avoided by using

Tutorial: Learn more about the **limitations of Beer's law** at www.tinyurl.com/skoogpia7

[4]For a discussion of the effects of stray radiation, see M. R. Sharpe, *Anal. Chem.*, **1984**, *56*, 339A, **DOI**: 10.1021/ac00266a880.

[5]E. J. Meehan, in *Treatise on Analytical Chemistry*, 2nd ed., P. J. Elving, E. J. Meehan, and I. M. Kolthoff, eds., Part I, Vol. 7, p. 73, New York: Wiley, 1981. For a spreadsheet approach to stray-light calculations, see S. R. Crouch and F. J. Holler, *Applications of Microsoft® Excel in Analytical Chemistry*, 3rd ed., pp. 320–322, Belmont, CA: Cengage Learning, 2017.

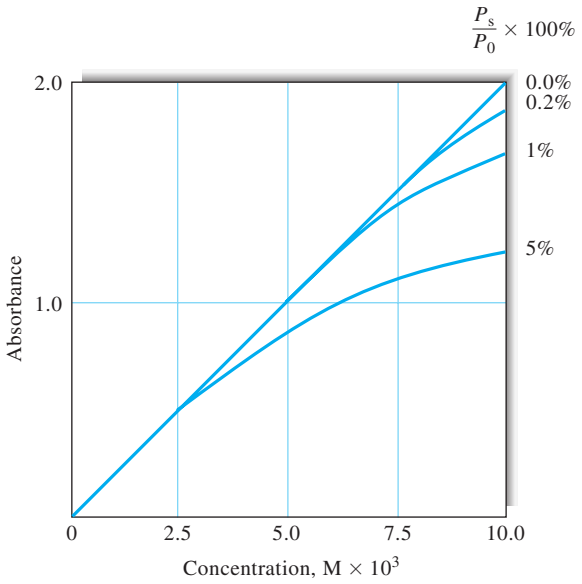

FIGURE 13-6 Apparent deviation from Beer's law brought about by various amounts of stray radiation. Note that the absorbance begins to level off with concentration at high stray-light levels. Stray light always limits the maximum absorbance that can be obtained because when the absorbance is high, the radiant power transmitted through the sample can become comparable to or lower than the stray-light level. P_s = stray radiation radiant power; P_0 = incident radiant power.

either carefully matched cells or a linear regression procedure to calculate both the slope and intercept of the calibration curve. In most cases linear regression is the best strategy because an intercept can also occur if the blank solution does not totally compensate for interferences. Another way to avoid the mismatched cell problem with single-beam instruments is to use only one cell and keep it in the same position for both blank and analyte measurements. After obtaining the blank reading, the cell is emptied by aspiration, washed, and filled with analyte solution.

13C THE EFFECTS OF INSTRUMENTAL NOISE ON SPECTROPHOTOMETRIC ANALYSES

The accuracy and precision of spectrophotometric analyses are often limited by the uncertainties or noise associated with the instrument.[6] A general discussion of instrumental noise and signal-to-noise optimization is found in Chapter 5.

[6]See L. D. Rothman, S. R. Crouch, and J. D. Ingle Jr., *Anal. Chem.*, **1975**, *47*, 1226, **DOI**: 10.1021/ac60358a029; J. D. Ingle Jr. and S. R. Crouch, *Anal. Chem.*, **1972**, *44*, 1375, **DOI**: 10.1021/ac60316a010; H. L. Pardue, T. E. Hewitt, and M. J. Milano, *Clin. Chem.*, **1974**, *20*, 1028, http://www.clinchem.org/content/20/8/1028.abstract; J. O. Erickson and T. Surles, *Amer. Lab.*, **1976**, *8* (6), 41; *Optimum Parameters for Spectrophotometry*, Santa Clara, CA: Agilent Technologies, Inc., 1977.

13C-1 Instrumental Noise as a Function of Transmittance

As was pointed out earlier, a spectrophotometric measurement entails three steps: a 0%T measurement or adjustment, a 100%T measurement, and a measurement of %T with the sample in the radiation path. The noise associated with each of these steps combines to give a net uncertainty for the final value obtained for T. The relationship between the noise encountered in the measurement of T and the resulting *concentration uncertainty* can be derived by writing Beer's law in the form

$$c = -\frac{1}{\varepsilon b}\log T = -\frac{0.434}{\varepsilon b}\ln T \qquad (13\text{-}10)$$

To relate the standard deviation in concentration σ_c to the standard deviation in transmittance σ_T, we proceed as in Section a1B-3, Appendix 1 by taking the partial derivative of this equation with respect to T, holding b and c constant. That is,

$$\frac{\partial c}{\partial T} = -\frac{0.434}{\varepsilon b T}$$

Application of Equation a1-29 (Appendix 1) gives

$$\sigma_c^2 = \left(\frac{\partial c}{\partial T}\right)^2 \sigma_T^2 = \left(\frac{-0.434}{\varepsilon b T}\right)^2 \sigma_T^2 \qquad (13\text{-}11)$$

Note that we use the population variance σ^2 instead of the sample variance s^2 when applying Equation a1-29. Dividing Equation 13-11 by the square of Equation 13-10 gives

$$\left(\frac{\sigma_c}{c}\right)^2 = \left(\frac{\sigma_T}{T \ln T}\right)^2$$

$$\frac{\sigma_c}{c} = \frac{\sigma_T}{T \ln T} = \frac{0.434\sigma_T}{T \log T} \qquad (13\text{-}12)$$

When there is a limited number of measurements and thus a small statistical sample, we replace the population standard deviations σ_c and σ_T with the sample standard deviations s_c and s_T (Section a1B-1, Appendix 1) and obtain

$$\frac{s_c}{c} = \frac{0.434 s_T}{T \log T} \qquad (13\text{-}13)$$

This equation relates the relative standard deviation in c (s_c/c) to the absolute standard deviation of the transmittance measurement (s_T). Experimentally, s_T can be evaluated by making, say, twenty replicate transmittance measurements ($N = 20$) of the transmittance of a solution in exactly the same way and substituting the data into Equation a1-10, Appendix 1.

Equation 13-13 shows that the uncertainty in a photometric concentration measurement varies nonlinearly with the magnitude of the transmittance. The situation is somewhat more complicated than is suggested by Equation 13-13, however, because the uncertainty s_T is also *dependent on T*.

TABLE 13-3 Types and Sources of Uncertainties in Transmittance Measurements

Category	Characterized by[a]	Typical Sources	Likely to Be Important In
Case I	$s_T = k_1$	Limited readout resolution	Inexpensive photometers and spectrophotometers having small meters or digital displays
		Heat detector Johnson noise	IR and near-IR spectrophotometers and photometers
		Dark current and amplifier noise	Regions where source intensity and detector sensitivity are low
Case II	$s_T = k_2\sqrt{T^2 + T}$	Photon detector shot noise	High-quality UV-visible spectrophotometers
Case III	$s_T = k_3 T$	Cell positioning uncertainties	High-quality UV-visible and IR spectrophotometers
		Source flicker	Inexpensive photometers and spectrophotometers

[a] k_1, k_2, and k_3 are constants for a given system.

13C-2 Sources of Instrumental Noise

In a detailed theoretical and experimental study, Rothman, Crouch, and Ingle have described several sources of instrumental uncertainties and shown their net effect on the precision of absorbance or transmittance measurements.[7] These uncertainties fall into one of three categories depending on how they are affected by the magnitude of the photocurrent and thus T. For Case I uncertainties, the precision is independent of T; that is, s_T is equal to a constant k_1. For Case II uncertainties, the precision is directly proportional to $\sqrt{T^2 + T}$. Finally, Case III uncertainties are directly proportional to T. Table 13-3 summarizes information about the sources of these three types of uncertainty and the kinds of instruments where each is likely to be encountered.

Case I: $s_T = k_1$

Case I uncertainties often appear in less expensive UV and visible spectrophotometers or photometers equipped with meters or digital readouts with limited resolution. For example, some digital instruments have 3½-digit displays. These can display the result to 0.1%T. Here, the readout resolution can limit the measurement precision such that the absolute uncertainty in T is the same from 0%T to 100%T. A similar limitation occurs with older analog instruments with limited meter resolution.

IR and near-IR spectrophotometers also exhibit Case I behavior. With these, the limiting random error usually arises from Johnson noise in the thermal detector. Recall (Section 5B-2) that this type of noise is independent of the magnitude of the photocurrent; indeed, fluctuations are observed even in the absence of radiation when there is essentially no net current.

Dark current and amplifier noise are usually small compared with other sources of noise in photometric and spectrophotometric instruments and become important only under conditions of low photocurrents where the lamp intensity or the transducer sensitivity is low. For example, such conditions are often encountered near the wavelength extremes for an instrument.

The precision of concentration data obtained with an instrument that is limited by Case I noise can be obtained directly by substituting an experimentally determined value for $s_T = k_1$ into Equation 13-13. Here, the precision of a particular concentration determination depends on the magnitude of T even though the instrumental precision is independent of T. The third column of Table 13-4 shows data obtained with Equation 13-13 when an absolute standard deviation s_T of ± 0.003, or $\pm 0.3\%T$, was assumed. Curve A in Figure 13-7 shows a plot of the data. Note that a minimum is reached at an absorbance of about 0.5. Note also that the relative concentration error rapidly rises at absorbances lower than about 0.1 and greater than about 1.0.

An uncertainty of 0.3%T is typical of many moderately priced spectrophotometers or photometers. With these instruments, concentration errors of 1% to 2% relative are to be expected if the absorbance of the sample lies between about 0.1 and 1.

Case II: $s_T = k_2\sqrt{T^2 + T}$

This type of uncertainty often limits the precision of the highest quality instruments. It has its origin in shot noise (Section 5B-2), which occurs whenever the current involves transfer of charge

Simulation: Learn more about the **effects of instrumental noise** at www.tinyurl.com/skoogpia7

[7] L. D. Rothman, S. R. Crouch, and J. D. Ingle Jr., *Anal. Chem.*, **1975**, *47*, 1226.

TABLE 13-4 Relative Precision of Concentration Measurements as a Function of Transmittance and Absorbance for Three Categories of Instrument Noise

		Relative Standard Deviation in Concentration[a]		
Transmittance, T	Absorbance, A	Case I Noise[b]	Case II Noise[c]	Case III Noise[d]
0.95	0.022	±6.2	±8.4	±25.3
0.90	0.046	±3.2	±4.1	±12.3
0.80	0.097	±1.7	±2.0	±5.8
0.60	0.222	±0.98	±0.96	±2.5
0.40	0.398	±0.82	±0.61	±1.4
0.20	0.699	±0.93	±0.46	±0.81
0.10	1.00	±1.3	±0.43	±0.56
0.032	1.50	±2.7	±0.50	±0.38
0.010	2.00	±6.5	±0.65	±0.2
0.0032	2.50	±16.3	±0.92	±0.23
0.0010	3.00	±43.4	±1.4	±0.19

[a] $(s_c/c) \times 100$.

[b] From Equation 13-13 with $s_T = k_1 = \pm 0.0030$.

[c] From Equation 13-14 with $k_2 = \pm 0.0030$.

[d] From Equation 13-15 with $k_3 = \pm 0.013$.

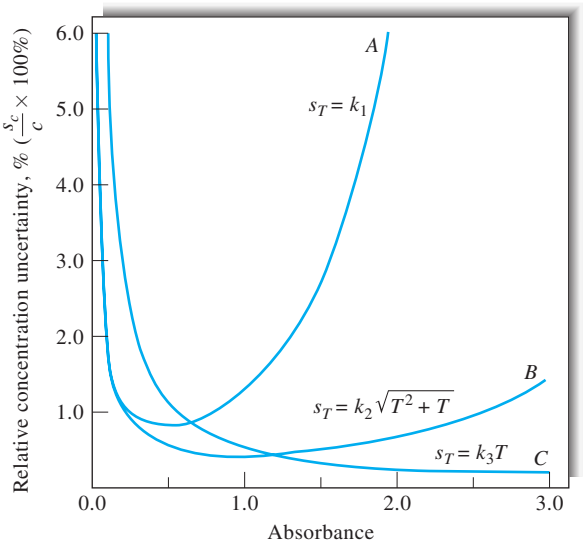

FIGURE 13-7 Relative concentration uncertainties arising from various categories of instrumental noise. *A*, case I; *B*, Case II; *C*, Case III. The data are taken from Table 13-4.

across a junction, such as the movement of electrons from the cathode to the anode of a photomultiplier tube. Here, an electric current results from a series of discrete events (emission of electrons from a cathode). The average number of these events per unit time is proportional to the photon flux. The frequency of events and thus the current is randomly distributed about the average value. The magnitude of the current fluctuations is proportional to the square root of current (see Equation 5-5). The effect of shot noise on s_c is derived by substituting s_T into Equation 13-13. Rearrangement leads to

$$\frac{s_c}{c} = \frac{0.434 k_2}{\log T}\sqrt{\frac{1}{T} + 1} \qquad (13\text{-}14)$$

The data in column 4 of Table 13-4 were calculated using Equation 13-14. Curve B in Figure 13-7 is a plot of such data. Note the much broader minimum in the concentration uncertainty. Note also that a large range of absorbances can be measured without the concentration error becoming greater than 1% to 2%. This increased range represents a major advantage of photon-type detectors over thermal types, which are represented by curve A in the figure. As with Johnson-noise-limited instruments, shot-limited instruments do not give very reliable concentration data at transmittances greater than 95% (or $A < 0.02$).

Case III: $s_T = K_3 T$

By substituting $s_T = k_3 T$ into Equation 13-13, we see that the relative standard deviation in concentration from this type of uncertainty is inversely proportional to the logarithm of the transmittance.

$$\frac{s_c}{c} = \frac{0.434 k_3}{\log T} \qquad (13\text{-}15)$$

Column 5 of Table 13-4 contains data obtained from Equation 13-15 when k_3 is assumed to have a value of 0.013, which

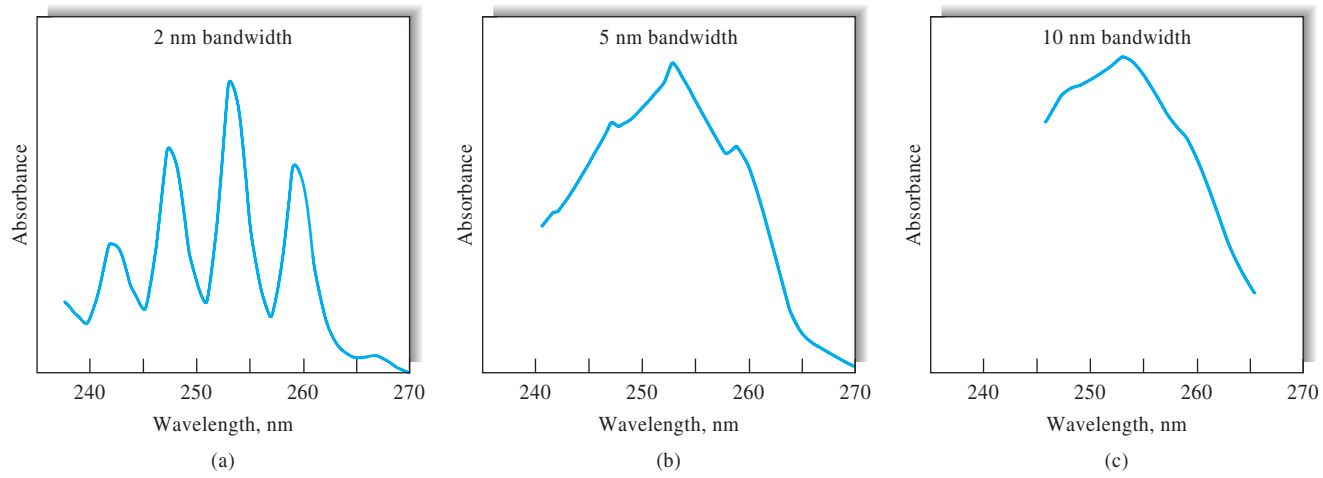

FIGURE 13-8 Effect of bandwidth on spectral detail for a sample of benzene vapor. Note that as the spectral bandwidth increases, the fine structure in the spectrum is lost. At a bandwidth of 10 nm, only a broad absorption band is observed.

approximates the value observed in the Rothman, Crouch, and Ingle study. The data are plotted as curve C in Figure 13-7. Note that this type of uncertainty is important at low absorbances (high transmittances) but approaches zero at high absorbances.[8]

One source of noise of this type is the slow drift in the radiant output of the source. This type of noise can be called *source flicker noise* (Section 5B-2). The effects of fluctuations in the intensity of a source can be minimized by the use of a constant-voltage power supply or a feedback system in which the source intensity is maintained at a constant level. Modern double-beam spectrophotometers (Sections 13D-2 and 13D-3) can also help cancel the effect of flicker noise. With many instruments, source flicker noise does not limit performance.

An important and widely encountered noise source, one that is proportional to transmittance, results from failure to position sample and reference cells reproducibly with respect to the beam during replicate transmittance measurements. All cells have minor imperfections. Because of these, reflection and scattering losses vary as different sections of the cell window are exposed to the beam; small variations in transmittance result. Rothman, Crouch, and Ingle have shown that this uncertainty often is the most common limitation to the accuracy of high-quality UV-visible spectrophotometers. It is also a serious source of uncertainty in IR instruments.

One method of reducing the effect of cell positioning with a double-beam instrument is to leave the cells in place during calibration and analysis. New standards and samples are then introduced after washing and rinsing the cell in place with a syringe. Care must be taken to avoid touching or jarring the cells during this process.

13C-3 Effect of Slit Width on Absorbance Measurements

As shown in Section 7C-3, narrow slit widths are required to resolve complex spectra.[9] For example, Figure 13-8 illustrates the loss of detail that occurs when slit widths are increased from small values on the left to larger values in the middle and right. In this example, the absorption spectrum of benzene vapor was obtained at slit settings that provided effective bandwidths of 1.6, 4, and 10 nm. For qualitative studies, the loss of resolution that accompanies the use of wider slits is often important because the details of spectra are useful for identifying species.

Figure 13-9 illustrates a second effect of slit width on spectra made up of narrow peaks. Here, the spectrum of a praseodymium chloride solution was obtained at slit widths of 1.0, 0.5, and 0.1 mm. Note that the peak absorbance values increase significantly (by as much as 70% in one instance) as the slit width decreases. At slit settings less than about 0.14 mm, absorbances were found to become independent of slit width. Careful inspection of Figure 13-8 reveals the same type of effect. In both sets of spectra, the areas under the individual peaks are the same, but wide slit widths result in broader peaks with lower maximum absorbances.

From both of these illustrations, we can conclude that quantitative measurement of narrow absorption bands requires using narrow slit widths or, alternatively, very reproducible slit-width

[8]For a spreadsheet approach to plotting the relative concentration errors for the cases considered here, see S. R. Crouch and F. J. Holler, *Applications of Microsoft® Excel in Analytical Chemistry*, 3rd ed., pp. 323–326, Belmont, CA: Cengage Learning, 2017.

[9]For a discussion of the effects of slit width on spectra, see *Optimum Parameters for Spectrophotometry*, Santa Clara, CA: Agilent Technologies, Inc., 1977; F. C. Strong III, *Anal. Chem.*, **1976**, *48*, 2155, **DOI**: 10.1021/ac50008a026; D. D. Gilbert, *J. Chem. Educ.*, **1991**, *68*, A278, **DOI**: 10.1021/ed068pA278.

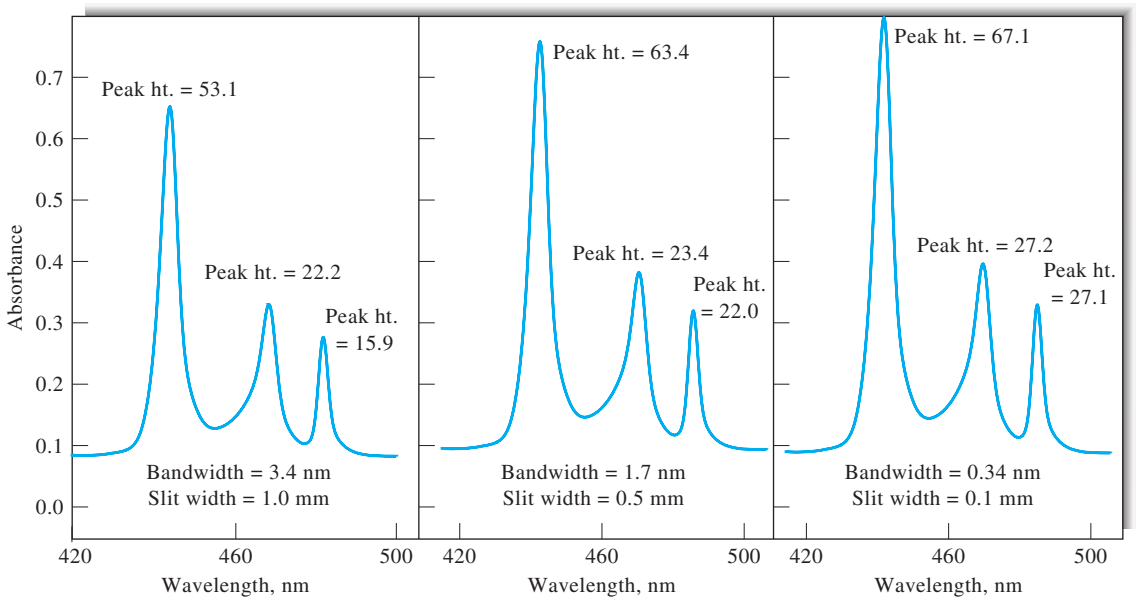

FIGURE 13-9 Effect of slit width (spectral bandwidth) on peak heights. Here, the sample was a solution of praseodymium chloride. Note that as the spectral bandwidth decreases by decreasing the slit width from 1.0 mm to 0.1 mm, the peak heights increase. (Data courtesy of Dr. Hilario López González, Departamento de Química, Instituto Nacional de Investigaciones Nucleares, México.)[10]

settings. Unfortunately, a decrease in slit width by a factor of 10 reduces the radiant power by a factor of 100 because the radiant power is proportional to the square of the slit width.[11] There is thus a trade-off between resolution and signal-to-noise ratio. Often, a compromise slit width must be chosen. The situation becomes particularly serious in spectral regions where the output of the source or the sensitivity of the detector is low. Under such circumstances, adequate signal-to-noise ratio may require slit widths large enough to result in partial or total loss of spectral fine structure.

In general, it is good practice to narrow slits no more than is necessary for resolution of the spectrum at hand. With a variable-slit spectrophotometer, proper slit adjustment can be determined by acquiring spectra at progressively narrower slits until maximum absorbances become constant. Generally, constant peak heights are observed when the effective bandwidth of the instrument is less than one tenth the full width at half maximum of the absorption band.

13C-4 Effect of Scattered Radiation at Wavelength Extremes of an Instrument

We have already noted that scattered radiation may cause instrumental deviations from Beer's law. When measurements are made at the wavelength extremes of an instrument, the effects of stray radiation may be even more serious and on occasion may lead to the appearance of false absorption bands. For example, consider an older visible spectrophotometer equipped with glass optics, a tungsten source, and a photovoltaic cell detector. At wavelengths below about 380 nm, the windows, cells, and prism begin to absorb radiation, thus reducing the energy reaching the transducer. The output of the source falls off rapidly in this region as does the sensitivity of the transducer. Thus, the total signal for the 100%T adjustment may be as low as 1% to 2% of that in the region between 500 and 650 nm.

The scattered radiation, however, is often made up of wavelengths to which the instrument is highly sensitive. Thus, the effects of stray radiation can be greatly enhanced. Indeed, in some instances the output signal produced by the stray radiation may exceed that produced by the monochromator output beam. In such cases, the component of the measured transmittance due to the stray radiation may be as large as or exceed the true transmittance.

An example of a false band appearing at the wavelength extremes of a visible-region spectrophotometer is shown in Figure 13-10. The spectrum of a solution of cerium(IV) obtained with a UV-visible spectrophotometer, sensitive in the region of 200 to 750 nm, is shown by curve *B*. Curve *A* is a spectrum of the same solution obtained with a simple visible spectrophotometer. The apparent maximum shown in curve *A* arises from the instrument responding to stray wavelengths longer than 400 nm. As can be seen in curve *B*, these longer wavelengths are not absorbed by the cerium(IV) ions. This same effect is sometimes observed with UV-visible instruments when attempts are made to measure absorbances at wavelengths lower than about 200 nm.

[10]R, González-Mendoza, H. López-González, y A. Rojas-Hernández, *J. Mex. Chem. Soc.* **2010**, *54*, 51, http://tinyurl.com/jhgl2wz.

[11]J. D. Ingle Jr. and S. R. Crouch, *Spectrochemical Analysis*, p. 366, Upper Saddle River, NJ: Prentice-Hall, 1988.

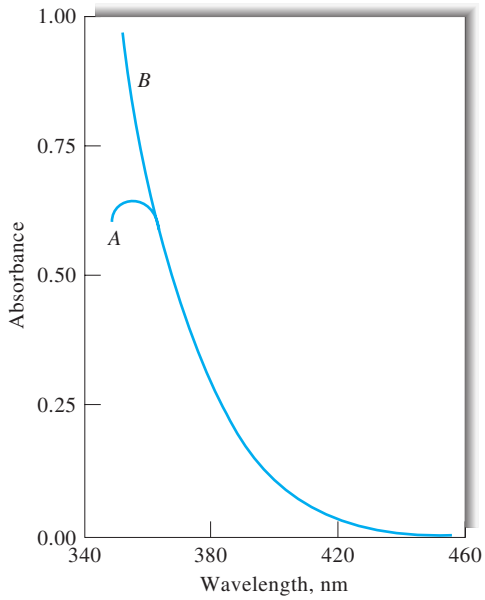

FIGURE 13-10 Spectrum of cerium(IV) obtained with a spectrophotometer having glass optics (*A*) and quartz optics (*B*). The false peak in *A* arises from transmission of stray radiation of longer wavelengths.

13D INSTRUMENTATION

Instruments for making molecular absorption measurements in the UV, visible, and near-IR regions are produced by dozens of companies. There are hundreds of instrument makes and models from which to choose. Some are simple and inexpensive (a few hundred dollars); others are complex, computer-controlled, scanning instruments costing $30,000 or more. The simpler instruments are often useful only in the visible region for quantitative measurements at a single wavelength. The more complex instruments can provide spectral scanning at selectable resolution, measurements in the UV as well as the visible regions, compensation for source intensity fluctuations, and several other features.[12]

13D-1 Instrument Components

Instruments for measuring the absorption of UV, visible, and near-IR radiation are made up of one or more (1) sources, (2) wavelength selectors, (3) sample containers, (4) radiation transducers, and (5) signal processors and readout devices. The design and performance of components (2), (4), and (5) were described in considerable detail in Chapter 7 and thus are not discussed further here. We will, however, consider briefly the characteristics of sources and sample containers for the region of 190 to 3000 nm.

[12]For an interesting discussion of commercial instruments for UV-visible absorption measurements, see R. Jarnutowski, J. R. Ferraro, and D. C. Lankin, *Spectroscopy*, **1992**, *7* (7), 22.

Sources

For the purposes of molecular absorption measurements, a continuum source is required whose radiant power does not change sharply over a considerable range of wavelengths.

Deuterium and Hydrogen Lamps. A continuum spectrum in the UV region is produced by electrical excitation of deuterium or hydrogen at low pressure. The mechanism by which a continuum spectrum is produced involves initial formation of an excited molecular species followed by dissociation of the excited molecule to give two atomic species plus a UV photon. The reactions for deuterium are

$$D_2 + E_e \rightarrow D_2^* \rightarrow D' + D'' + h\nu$$

where E_e is the electrical energy absorbed by the molecule and D_2^* is the excited deuterium molecule. The energetics for the overall process can be represented by the equation

$$E_e = E_{D_2^*} = E_{D'} + E_{D''} + h\nu$$

Here, $E_{D_2^*}$ is the fixed quantized energy of D_2^* whereas $E_{D'}$ and $E_{D''}$ are the kinetic energies of the two deuterium atoms. The sum of $E_{D'}$ and $E_{D''}$ can vary continuously from zero to $E_{D_2^*}$; thus, the energy and the frequency of the photon can also vary continuously. That is, when the two kinetic energies are by chance small, $h\nu$ will be large, and conversely. The result is a true continuum spectrum from about 160 nm to the beginning of the visible region, as shown in Figure 13-11b.

Most modern lamps of this type contain deuterium instead of hydrogen and are of a low-voltage type in which an arc is formed between a heated, oxide-coated filament and a metal electrode (see Figure 13-11a). The heated filament provides electrons to maintain a direct current when about 40 V is applied between the filament and the electrode. A regulated power supply is required for constant intensities.

An important feature of deuterium and hydrogen discharge lamps is the shape of the aperture between the two electrodes, which constricts the discharge to a narrow path. As a result, an intense ball of radiation about 1 to 1.5 mm in diameter is produced. Deuterium gives a somewhat larger and brighter ball than hydrogen, which accounts for the widespread use of deuterium.

Both deuterium and hydrogen lamps produce outputs in the range of 160–800 nm. In the UV region (190–400 nm), a continuum spectrum exists as can be seen in Figure 13-11b. At longer wavelengths (>400 nm), the spectra from these lamps are no longer continua, but consist of emission lines and bands superimposed on a weak continuum. For many applications, the line or band emission represents a nuisance. However, some modern array-detector instruments use a deuterium source at wavelengths as long as 800 nm. With these, the array can be exposed for longer times to compensate for the low source intensity in the visible region. Because the entire source spectrum is readily obtained with a solvent blank and then with the sample, the presence of emission lines does not interfere with calculation of

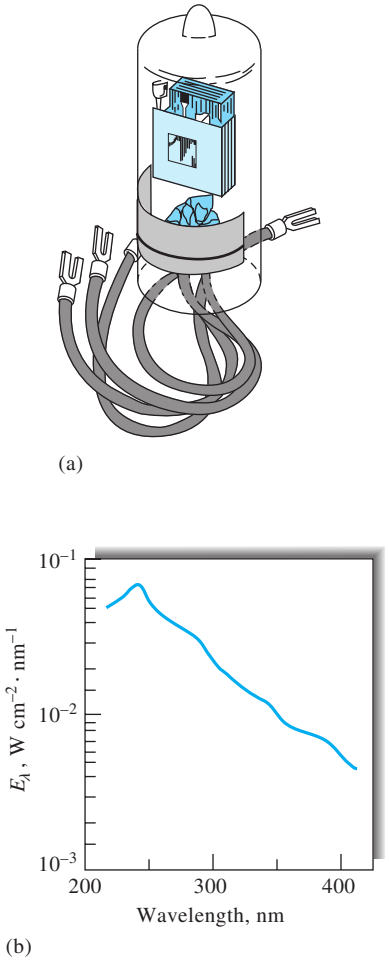

FIGURE 13-11 (a) A deuterium lamp of the type used in spectrophotometers and (b) its spectrum. The plot is of irradiance E_λ (proportional to radiant power) versus wavelength. Note that the maximum intensity occurs at ~225 nm. Typically, instruments switch from deuterium to tungsten at ~350 nm.

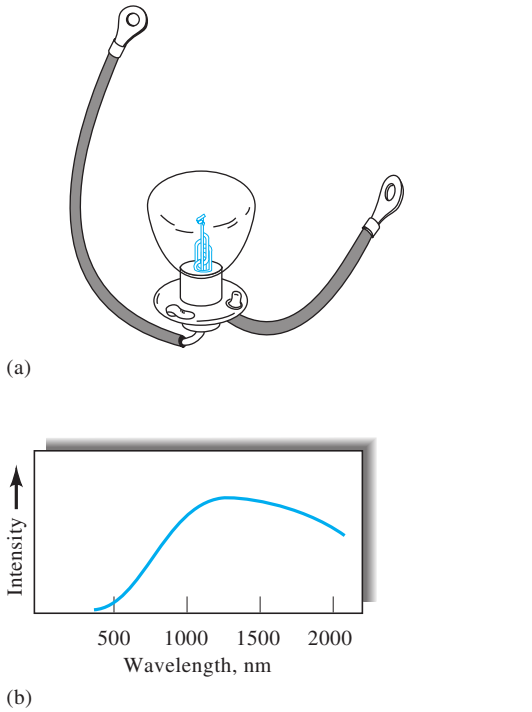

FIGURE 13-12 (a) A tungsten lamp of the type used in spectroscopy and its spectrum (b). Intensity of the tungsten source is usually quite low at wavelengths shorter than about 350 nm. Note that the intensity reaches a maximum in the near-IR region of the spectrum (~1200 nm in this case).

the absorption spectrum. The line emission has also been used for wavelength calibration of absorption instruments.

Quartz windows must be used in deuterium and hydrogen lamps because glass absorbs strongly at wavelengths less than about 350 nm. Although the deuterium lamp continuum spectrum extends to wavelengths as short as 160 nm, the useful lower limit is about 190 nm because of absorption by the quartz windows.

Tungsten Filament Lamps. The most common source of visible and near-IR radiation is the tungsten filament lamp. The energy distribution of this source approximates that of a blackbody (see Figure 6-22) and is thus temperature dependent. In most absorption instruments, the operating filament temperature is 2870 K; the bulk of the energy is thus emitted in the IR region. A tungsten filament lamp is useful for the wavelength region between 350 and 2500 nm. Figure 13-12 shows a typical tungsten lamp and its spectrum. Absorption of radiation by the glass envelope that houses the filament imposes the lower wavelength limit.

In the visible region, the energy output of a tungsten lamp varies approximately as the fourth power of the operating voltage. Precise voltage control is therefore required for a stable radiation source. Electronic voltage regulators or feedback-controlled power supplies are usually needed to obtain the required stability.

Tungsten-halogen lamps, also called quartz-halogen lamps, contain a small quantity of iodine within a quartz envelope that houses the tungsten filament. Quartz allows the filament to be operated at a temperature of about 3500 K, which leads to higher intensities and extends the range of the lamp well into the UV region. The lifetime of a tungsten-halogen lamp is more than double that of the ordinary lamp. This added life results from the reaction of the iodine with gaseous tungsten that forms by sublimation and ordinarily limits the life of the filament; the product is the volatile WI_2. When molecules of this compound strike the filament, decomposition occurs, which redeposits tungsten. Tungsten-halogen lamps are significantly more efficient and extend the output wavelength range well into the UV. For these reasons, they are found in many modern spectroscopic instruments.

Light-Emitting Diodes. Light-emitting diodes (LEDs) are used as sources in some absorption spectrometers. An LED is a *pn*-junction device that, when forward biased, produces radiant energy. Diodes made from gallium aluminum arsenide (λ_m = 900 nm), gallium arsenic phosphide (λ_m = 650 nm), gallium phosphide (λ_m = 550 nm), gallium nitride (λ_m = 465 nm), and indium gallium nitride (λ_m = 450 nm) are widely available. Mixtures of these compounds are used to shift the wavelength maximum to anywhere in the region of 375 nm to 1000 nm or more. LEDs produce a spectral continuum over a narrow wavelength range. Typically, the full width at half maximum of an LED is 20 to 50 nm. As spectroscopic sources, LEDs can be used as "semimonochromatic" sources or in conjunction with interference filters to further narrow the spectral output. They can be operated in a continuous mode or in a pulsed mode.

"White" LEDs are also available in which the light from a blue LED (InGaN) strikes a phosphor, which emits a spectral continuum typically in the range of 400–800 nm. Such LEDs are being used to make lighting products such as flashlights. They have the advantage of long lifetimes and a smaller environmental impact than tungsten filament lamps.

Xenon Arc Lamps. The xenon arc lamp produces intense radiation by the passage of current through an atmosphere of xenon. The spectrum is a continuum over the range between about 200 and 1000 nm, with the peak intensity occurring at about 500 nm (see Figure 6-22). In some instruments, the lamp is operated intermittently by regular discharges from a capacitor; high intensities are obtained.

Sample Containers

In common with the other optical elements of an absorption instrument, the cells, or cuvettes, that hold the sample and solvent must be constructed of a material that passes radiation in the spectral region of interest. Thus, as shown in Figure 7-2a, quartz or fused silica is required for work in the UV region (below 350 nm). Both of these substances are transparent throughout the visible and near-IR regions to about 3 μm. Silicate glasses can be used in the region between 350 and 2000 nm. Plastic containers are also used in the visible region.

The best cells minimize reflection losses by having windows that are perfectly normal to the direction of the beam. The most common path length for studies in the UV and visible regions is 1 cm. Matched, calibrated cells of this size are available from several commercial sources. Other path lengths, from 0.1 cm (and shorter) to 10 cm, can also be purchased. Transparent spacers for shortening the path length of 1-cm cells to 0.1 cm are also available.

Cylindrical cells are sometimes used in the UV and visible regions because they are inexpensive. Special care must be taken to reproduce the position of the cell with respect to the beam; otherwise, variations in path length and reflection losses at the curved surfaces can cause significant errors.

The quality of absorbance data depends critically on the way the cells are used and maintained. Fingerprints, grease, or other deposits on the walls markedly alter the transmission characteristics of a cell. Thus, it is essential to clean cells thoroughly before and after use. The surface of the windows must not be touched during handling. Matched cells should never be dried by heating in an oven or over a flame—such treatment may cause physical damage or a change in path length. The cells should be regularly calibrated against each other with an absorbing solution.

13D-2 Types of Instruments

In this section, we consider four general types of spectroscopic instruments: (1) single beam, (2) double beam in space, (3) double beam in time, and (4) multichannel.

Single-Beam Instruments

Figure 13-13a is a schematic of a single-beam instrument for absorption measurements. It consists of a tungsten or deuterium lamp, a filter or a monochromator for wavelength selection, matched cells that can be placed alternately in the radiation beam, one of the transducers described in Section 7E, an amplifier, and a readout device. Normally, a single-beam instrument requires a stabilized voltage supply to avoid errors resulting from changes in the beam intensity during the time required to make the 100%T measurement and determine %T for the analyte.

Single-beam instruments vary widely in their complexity and performance characteristics. The simplest and least expensive consists of a battery-operated tungsten bulb as the source, a set of glass filters for wavelength selection, test tubes for sample holders, a photovoltaic cell as the transducer, and an analog meter as the readout device. At the other extreme are sophisticated, computer-controlled instruments with a range of 200 to 1000 nm or more. These spectrophotometers have interchangeable tungsten and deuterium lamp sources, use rectangular silica cells, and are equipped with a high-resolution grating monochromator with variable slits. Photomultiplier tubes are used as transducers, and the output is often digitized, processed, and stored in a computer so that it can be printed or plotted in several forms.

Double-Beam Instruments

Many modern photometers and spectrophotometers are based on a double-beam design. Figure 13-13b illustrates a double-beam-in-space instrument in which two beams are formed in space by a V-shape mirror called a *beamsplitter*. One beam passes through the reference solution to a photodetector, and the second simultaneously traverses the sample to a second,

Exercise: Learn more about **single-beam, double-beam, and multichannel instruments** at www.tinyurl.com/skoogpia7

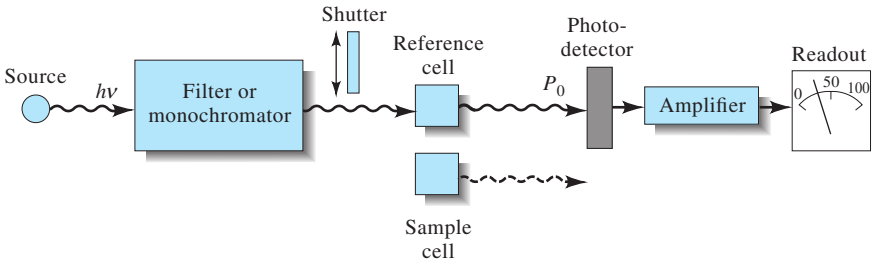

(a)

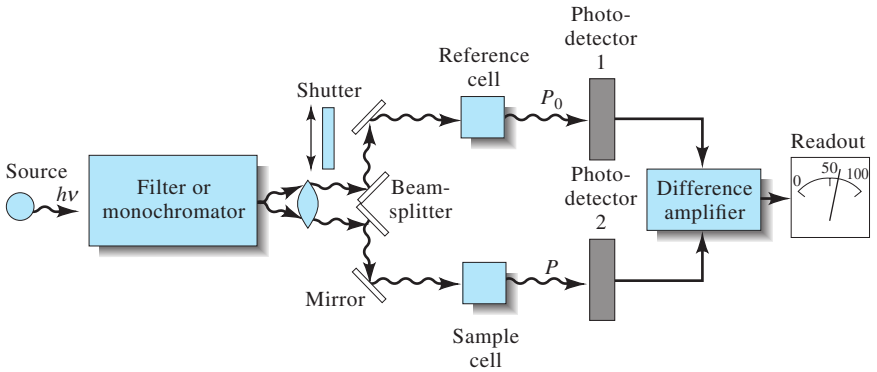

(b)

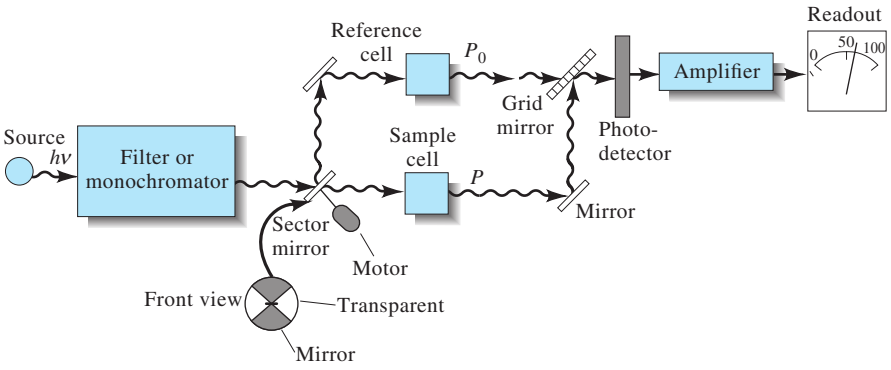

(c)

FIGURE 13-13 Instrumental designs for UV-visible photometers or spectrophotometers. In (a), a single-beam instrument is shown. Radiation from the filter or monochromator passes through either the reference cell or the sample cell before striking the photodetector. In (b), a double-beam-in-space instrument is shown. Here, radiation from the filter or monochromator is split into two beams that simultaneously pass through the reference and sample cells before striking two matched photodetectors. In the double-beam-in-time instrument (c), the beam is alternately sent through reference and sample cells before striking a single photodetector. Only a matter of milliseconds separate the beams as they pass through the two cells.

matched detector. The two outputs are amplified, and their ratio (or the logarithm of their ratio) is determined electronically or by a computer and displayed by the readout device. With manual instruments, the measurement is a two-step operation involving first the zero adjustment with a shutter in place between selector and beamsplitter. In the second step, the shutter is opened and the transmittance or absorbance is displayed directly.

The second type of double-beam instrument is illustrated in Figure 13-13c. Here, the beams are separated in time by a rotating sector mirror that directs the entire beam from the monochromator first through the reference cell and then through the sample cell. The pulses of radiation are recombined by another sector mirror, which transmits one pulse and reflects the other to the transducer. As shown by the insert labeled "front

view" in Figure 13-13c, the motor-driven sector mirror is made up of pie-shape segments, half of which are mirrored and half of which are transparent. The mirrored sections are held in place by blackened metal frames that periodically interrupt the beam and prevent its reaching the transducer. The detection circuit is programmed to use these periods to perform the dark-current adjustment. The double-beam-in-time approach is generally preferred because of the difficulty in matching the two detectors needed for the double-beam-in-space design.

Double-beam instruments offer the advantage that they compensate for all but the most short-term fluctuations in the radiant output of the source as well as for drift in the transducer and amplifier. They also compensate for wide variations in source intensity with wavelength (see Figures 13-11 and 13-12). Furthermore, the double-beam design lends itself well to the continuous recording of transmittance or absorbance spectra.

Multichannel Instruments

A new type of spectrophotometer appeared on the market in the early 1980s that was based on one of the array detectors (photodiode array or linear charge-coupled-device [CCD] array) described in Section 7E. These instruments are usually of the single-beam design shown in Figure 13-14. With multichannel systems, the dispersive system is a grating spectrograph placed after the sample or reference cell. The array detector is placed in the focal plane of the spectrograph, where the dispersed radiation strikes it.

The photodiode array discussed in Section 7E-3, consists of a linear array of several hundred photodiodes (256, 512, 1024, 2048) that have been formed along the length of a silicon chip. Typically, the chips are 1 to 6 cm long, and the widths of the individual diodes are 15 to 50 μm (see Figure 13-15). Linear CCD arrays typically consist of 2048 elements, with each element being ~14 μm wide. The linear CCD is substantially more sensitive than the photodiode array and behaves much like a linear array of miniature photomultiplier tubes.

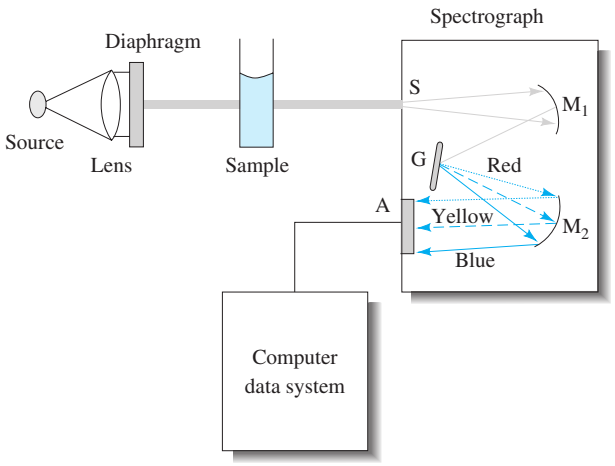

FIGURE 13-14 Diagram of a multichannel spectrometer based on a grating spectrograph with an array detector. Radiation from the tungsten or deuterium source is made parallel and reduced in size by the lens and diaphragm. Radiation transmitted by the sample enters the spectrograph through slit S. Collimating mirror M_1 makes the beam parallel before it strikes the grating G. The grating disperses the radiation into its component wavelengths, which are then focused by focusing mirror M_2 onto the photodiode or CCD array A. The output from the array detector is then processed by the computer data system.

FIGURE 13-15 Diode arrays of various sizes. (Courtesy of Hamamatsu Photonics, Bridgewater, NJ.)

With single-beam designs, the array dark current is measured and stored in computer memory. Next, the spectrum of the source is obtained and stored in memory after dark-current subtraction. Finally, the raw spectrum of the sample is obtained and, after dark-current subtraction, the sample values are divided by the source values at each wavelength and processed to give absorbances. Multichannel instruments can also be configured as double-beam-in-time spectrophotometers.

The spectrograph entrance slit of multichannel instruments is usually variable from about the width of one of the array elements to many times wider. Some spectrometers have no entrance slit but instead use a fiber optic as the entrance aperture. Multichannel spectrometers using both photodiode arrays and CCD arrays are capable of obtaining an entire spectrum in a few milliseconds. With array detectors the light can be integrated on a chip or multiple scans can be averaged in computer memory to enhance the signal-to-noise ratio.

A multichannel instrument is a powerful tool for studies of transient intermediates in moderately fast reactions, for kinetic studies, and for the qualitative and quantitative determination of the components exiting from a liquid chromatographic column or a capillary electrophoresis column. They are also useful for general-purpose scanning experiments. Some have the software necessary to analyze the time dependence at four or more wavelengths for kinetic studies.

Complete general-purpose array-detector-based spectrophotometers are available commercially for less than $10,000 and up. Several instrument companies combine array-detector systems with fiber-optic probes that transport the light to and from the sample.

13D-3 Some Typical Instruments

In the sections that follow, some typical photometers and spectrophotometers are described. The instruments were chosen to illustrate the wide variety of design variables that are encountered.

Photometers

Photometers provide simple, relatively inexpensive tools for performing absorption measurements. Filter photometers are often more convenient and more rugged and are easier to maintain and use than the more sophisticated spectrophotometers. Furthermore, photometers characteristically have high radiant energy throughputs and thus good signal-to-noise ratios even with relatively simple and inexpensive transducers and circuitry. Filter photometers are particularly useful in portable instruments intended for field use or for use in measuring the absorbances of flowing streams. These photometers are also used for quantitative determinations in clinical laboratories.

Visible Photometers. Figure 13-16 presents schematics for two visible photometers or colorimeters. The upper figure illustrates a single-beam, direct-reading instrument consisting of a tungsten filament lamp or an LED as a source, a lens to provide a parallel beam of light, a filter, and a photodiode transducer. The current produced by the photodiode is processed with electronics or a computer to give a direct readout in absorbance (shown) or, in some cases, transmittance. For most instruments, the dark current (0%T) is obtained by blocking the light beam with a shutter. The 100%T (0 A) is adjusted with solvent or a reagent blank in the light path. With some instruments, the 0 A adjustment is made by changing the voltage applied to the lamp. In others, the aperture size of a diaphragm located in the light path is altered. The sample is then inserted into the light path. Most modern colorimeters store the photodiode signal for the reference (proportional to P_0) and compute the ratio of this signal to the photodiode signal for the sample (proportional to the radiant power P). The absorbance is calculated as the logarithm of the ratio of these signals (Equation 13-3).

A modern LED-based photometer is shown in Figure 13-17. With some instruments, the wavelength is automatically changed by changing the LED or filter. Some instruments are made to operate at only one fixed wavelength. Calibration can be accomplished with two or more standards. The instrument shown is of the fixed-wavelength design with a bandwidth of 15 nm. Wavelengths of 420, 450, 476, 500, 550, 580, 600, and 650 nm are available.

Figure 13-16b is a schematic representation of a double-beam photometer used to measure the absorbance of a sample in a flowing stream. Here, the light beam is split by a two-branched (bifurcated) fiber optic, which transmits about 50% of the radiation striking it in the upper arm and about 50% in the lower arm. One beam passes through the sample, and the other passes through the reference cell. Filters are placed after the cells before

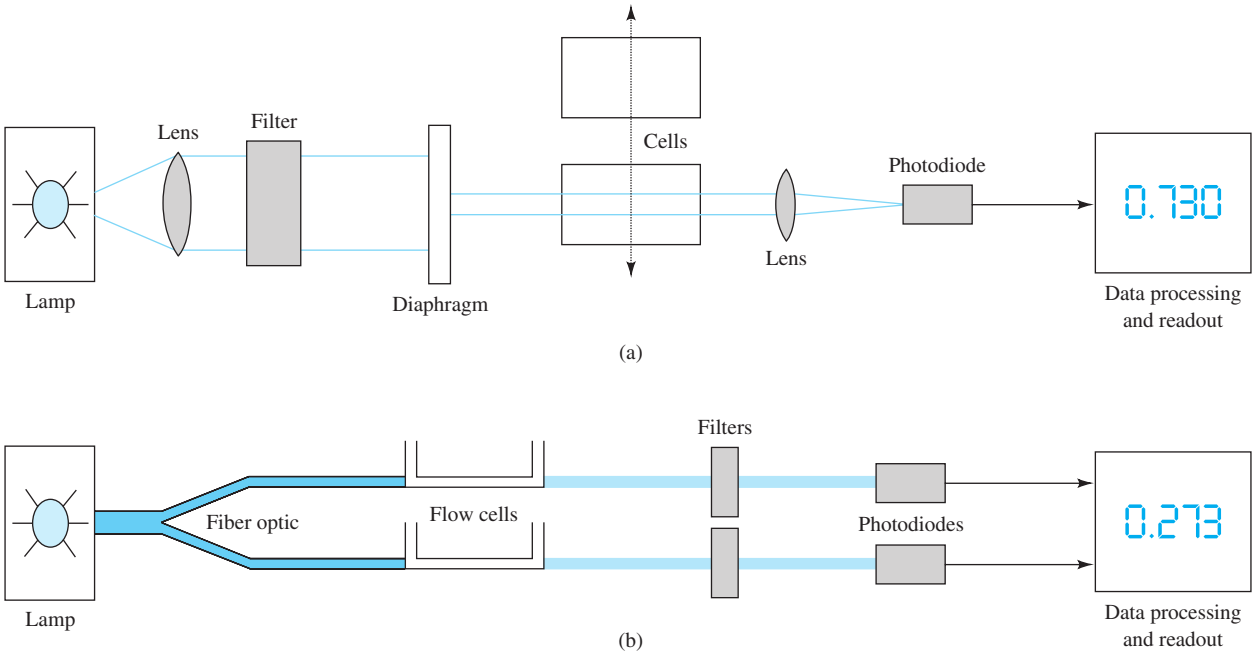

FIGURE 13-16 Single-beam photometer (a) and double-beam photometer for flow analysis (b). In the single-beam system, the reference cell is first placed in the light path and later replaced by the sample cell. In the double-beam system (b), a fiber optic splits the beam into two branches. One passes through the sample cell and the other through the reference cell. Two matched photodiodes are used in this double-beam-in-space arrangement.

FIGURE 13-17 Photograph of a simple LED-based colorimeter. (Hach Company, USA.)

the photodiode transducers. Note that this is the double-beam-in-space design, which requires photodiodes with nearly identical response. The electrical outputs from the two photodiodes are converted to voltages, and the signals are processed to give a readout proportional to absorbance.

Probe-Type Photometers. Figure 13-18 shows a photograph and a schematic of an interesting, commercially available, dipping-type photometer, which uses an optical fiber to transmit light from a source to a layer of solution lying between the glass seal at the end of the fiber and a mirror. The reflected radiation from the latter passes to a photodiode detector via a second glass fiber. The photometer uses an amplifier with an electronic chopper synchronized with the light source; as a result, the photometer does not respond to extraneous radiation. Filter options include "drop-in" filters and a filter wheel with six interference filters for selected applications. Custom filters are also available. Probe tips are manufactured from stainless steel, Swagelok® Stainless Steel, Pyrex®, and Acid-resistant Lexan® Plastic. Light path lengths that vary from 1 mm to 10 cm are available.

Absorbance is measured by first dipping the probe into the solvent and then into the solution to be measured. The device is particularly useful for photometric titrations (Section 14E).

Filter Selection. General-purpose photometers are supplied with several filters, each of which transmits a different portion of the visible spectrum. Selection of the proper filter for a given application is important because the sensitivity of the measurement directly depends on the choice. Usually for a new analytical method, the absorption spectrum of the solution to be analyzed is taken on a scanning spectrophotometer. The filter that most closely matches the wavelength of maximum absorption is then chosen. In some cases, measurements are made away from the absorption maximum to minimize interferences. Whenever possible, measurements are made near the absorption maximum to minimize Beer's law deviations due to polychromatic radiation (Section 13B-2).

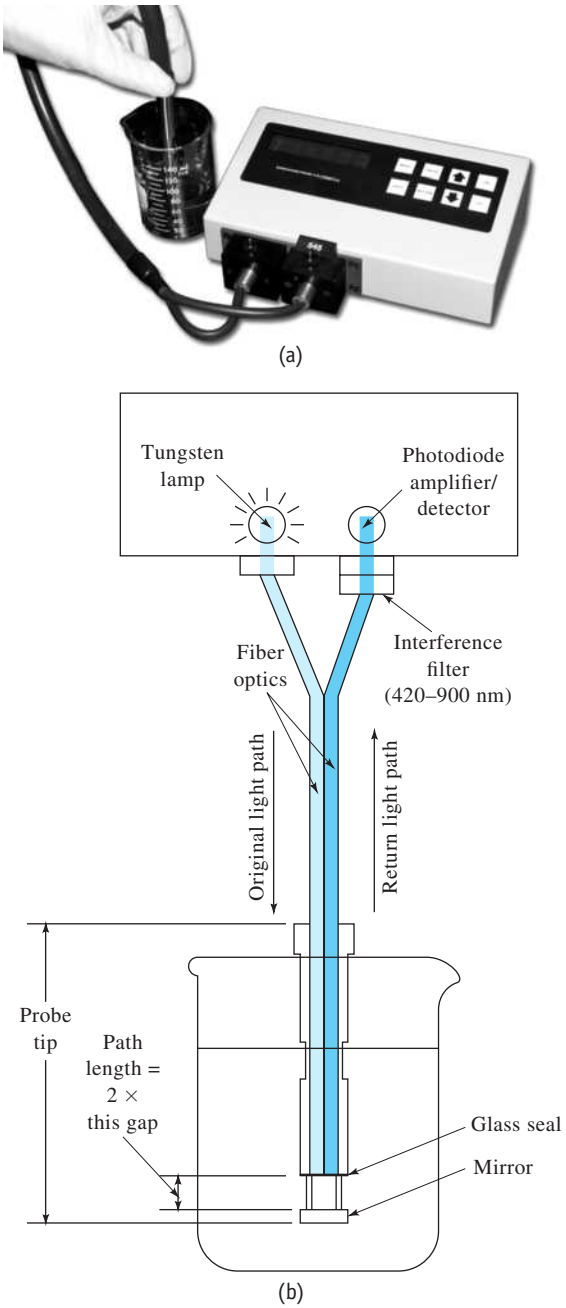

FIGURE 13-18 Photograph (a) and schematic diagram (b) of a probe-type photometer. (Courtesy of Metrohm USA, Riverview, FL.)

When a spectrophotometer is not available to aid in filter selection, a filter can be chosen by remembering that the color of the light absorbed is the complement of the color of the solution itself.

A solution appears red, for example, because it transmits the red portion of the spectrum but absorbs the green. It is the intensity of radiation in the green that varies with concentration. Hence, a green filter should be used. In general, the most suitable filter will be the color complement of the solution being analyzed.

Ultraviolet Absorption Photometers

UV photometers often serve as detectors in high-performance liquid chromatography. In this application, a mercury vapor lamp usually serves as a source, and the emission line at 254 nm is isolated by filters. This type of detector is described briefly in Section 28C-6.

UV photometers are also available for continuously monitoring the concentration of one or more constituents of gas or liquid streams in industrial plants. The instruments are double beam in space (see Figure 13-16b) and often use one of the emission lines of mercury, which has been isolated by a filter system. Typical applications include the determination of low concentrations of phenol in wastewater; monitoring the concentration of chlorine, mercury, or aromatics in gases; and the determination of the ratio of hydrogen sulfide to sulfur dioxide in the atmosphere.

Spectrophotometers

Numerous spectrophotometers are available from commercial sources. Some have been designed for the visible region only; others are applicable in the UV and visible regions. A few have measuring capabilities from the UV through the near IR (190 to 3000 nm).

Instruments for the Visible Region. Several spectrophotometers designed to operate within the wavelength range of about 380 to 800 nm are available from commercial sources. These instruments are frequently simple, single-beam grating instruments that are relatively inexpensive (less than $1000 to perhaps $3000), rugged, and readily portable. At least one is battery operated and light and small enough to be handheld. The most common application of these instruments is for quantitative analysis, although several produce good absorption spectra as well.

Figure 13-19 shows a simple and inexpensive spectrophotometer, the Spectronic 20. The original version of this instrument first appeared in the market in the mid-1950s. The modified version shown in the figure is still widely available along with the newer Spectronic 200. More of these instruments are currently in use throughout the world than any other single spectrophotometer model. The instrument owes its popularity, particularly as a teaching tool, to its relatively low cost, its ruggedness, and its satisfactory performance characteristics.

The Spectronic instruments use a tungsten or tungsten-halogen light source, which is operated by a stabilized power supply that provides radiation of constant intensity. After diffraction by a simple reflection grating, the radiation passes through the sample or reference cuvettes to a solid state detector. The Spectronic 20 reads out in transmittance or in absorbance on an LED display or, in the analog model, in transmittance on a meter. The Spectronic 200 has an LCD digital display.

The Spectronic 20 is equipped with an occluder, a vane that automatically falls between the beam and the detector whenever the cuvette is removed from its holder. The 0%T adjustment is made with the curvette removed. As shown in Figure 13-20, the light-control device in the Spectronic 20 consists of a V-shape slot that can be moved in or out of the beam to set the meter to 100%T.

To obtain a percent transmittance reading with the Spectronic 20, the digital readout is first zeroed with the sample compartment empty so that the occluder blocks the beam and no radiation reaches the detector. This process is called the *0%T calibration*, or *adjustment*. A cell containing the blank (often the solvent) is then inserted into the cell holder, and the pointer is brought to the 100%T mark by adjusting the position of the light-control aperture and thus the amount of light reaching the detector. This adjustment is called the *100%T calibration*, or *adjustment*. Finally the sample is placed in the cell compartment, and the percent transmittance or the absorbance is read directly from the LED display.

The Spectronic 200 measures 0%T automatically at start-up and can record 100%T over its entire wavelength range. A spectral scanning mode allows entire spectra to be recorded.

The Spectronic 20 was discontinued in 2011 and replaced by the Spectronic 200. This newer instrument has a spectral range of 340–1000 nm versus 400–900 nm for the Spectronic 20. The Spectronic 200 has a spectral bandwidth of 4 nm instead of the 20 nm bandwidth of the Spectronic 20. The newer instrument accommodates square cuvettes as well as the traditional test tubes of the Spectronic 20. It uses a reverse geometry compared to the original instrument and a CCD array detector. Other specifications include a wavelength accuracy of ± 2 nm for the 200 (± 2.5 nm for the Spectronic 20), and a photometric accuracy of ± 0.05 absorbance units at 1.0 A for the 200 versus $\pm 4\%T$ for the Spectronic 20. The Spectronic 200 has an emulation mode in which it provides many of the same operations as the legacy instruments so that methods and procedures developed previously can be used.

Single-Beam Instruments for the Ultraviolet-Visible Region. Several instrument manufacturers offer nonrecording single-beam instruments that can be used for both UV and visible measurements. The lower wavelength extremes for these instruments vary from 190 to 210 nm, and the upper from 800 to 1000 nm. All are equipped with interchangeable tungsten and hydrogen or deuterium lamps. Most use photomultiplier tubes or photodiodes as transducers and gratings for dispersion. Digital readouts are now standard on almost all these spectrophotometers. The prices for these instruments range from $2000 to $8000.

As might be expected, performance specifications vary considerably among instruments and are related, at least to some degree, to instrument price. Typically, bandwidths vary from 2 to 8 nm; wavelength accuracies of ± 0.5 to ± 2 nm are reported.

The optical designs for the various grating instruments do not differ greatly from those shown in Figures 13-13a and 13-19. One manufacturer, however, uses a concave rather

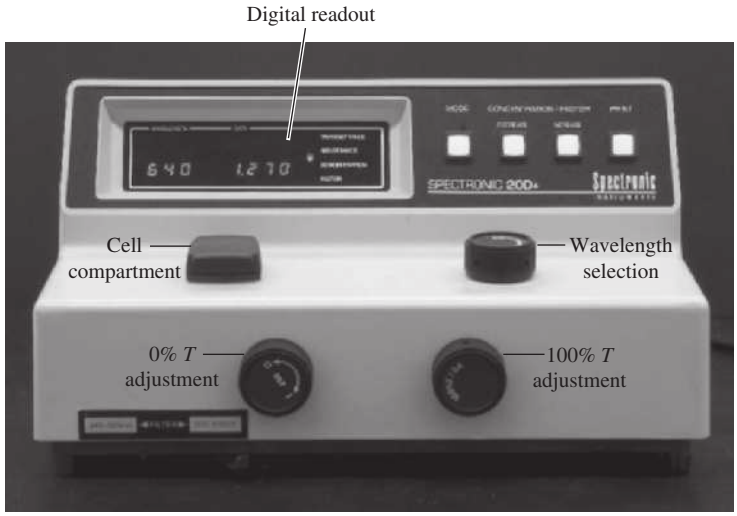

(a)

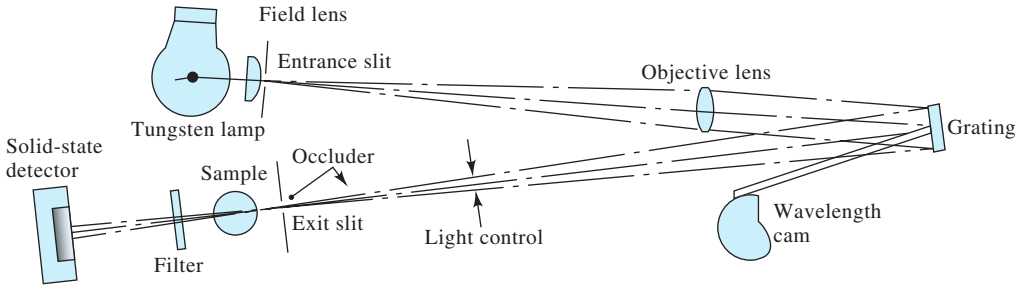

(b)

FIGURE 13-19 (a) The Spectronic 20 spectrophotometer and (b) its optical diagram. Radiation from the tungsten filament source passes through an entrance slit into the monochromator. A reflection grating diffracts the radiation, and the selected wavelength band passes through the exit slit into the sample chamber. A solid-state detector converts the light intensity into a related electrical signal that is amplified and displayed on a digital readout. The newer Spectronic 200 has a reverse optical path. (Courtesy of Thermo Electron Corp., Madison, WI.)

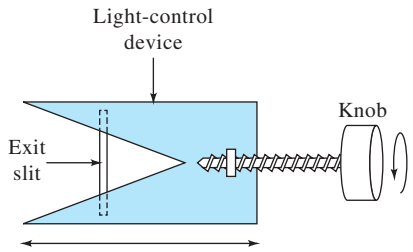

FIGURE 13-20 End view of the exit slit of the Spectronic 20 spectrophotometer pictured in Figure 13-19.

than a plane grating; a simpler and more compact design results. Holographic gratings are now standard in many spectrophotometers.

Single-Beam Computerized Spectrophotometers. Several manufacturers offer computerized, recording, single-beam spectrophotometers, which operate in the UV-visible range. With these instruments, a wavelength scan is first performed with the reference solution in the beam path. The resulting transducer output is digitized and stored in computer memory. Samples are then scanned and absorbances calculated with the aid of the stored reference solution data. The complete spectrum is displayed within a few seconds of data acquisition. Because the reference and sample spectra are taken at different times, it is necessary that source intensity remain constant. The computer associated with these instruments provides several options with regard to data processing and presentation such as log absorbance, transmittance, derivatives, overlaid spectra, repetitive scans, concentration calculations, peak location and height determinations, and kinetic measurements.

As noted earlier, single-beam instruments have the inherent advantages of greater energy throughput, superior signal-to-noise ratios, and less cluttered sample compartments. On the other hand, the double-beam instruments described next provide better baseline flatness and long-term stability than do the single-beam systems. The highest-quality spectrophotometers still use the double-beam design.

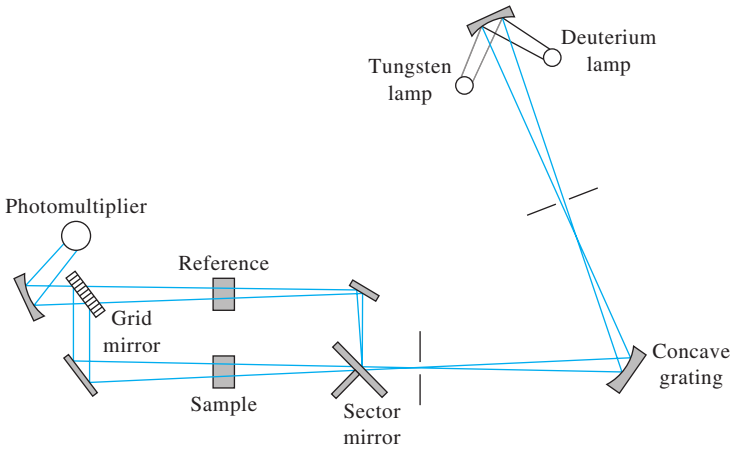

FIGURE 13-21 Schematic of a typical manual double-beam spectrophotometer for the UV-visible region.

Double-Beam Instruments. Numerous double-beam spectrophotometers for the UV-visible region of the spectrum are now available. Generally, these instruments are more expensive than their single-beam counterparts, with the nonrecording variety ranging from about less than $10,000 to more than $50,000.

Figure 13-21 shows construction details of a typical, relatively inexpensive, manual, double-beam UV-visible spectrophotometer. In this instrument, the radiation is dispersed by a concave grating, which also focuses the beam on a rotating sector mirror. The instrument design is similar to that shown in Figure 13-13c.

The instrument has a wavelength range of 195 to 850 nm, a bandwidth of 4 nm, a photometric accuracy of 0.5%T, and a reproducibility of 0.2% A; stray radiation is less than 0.1% of P_0 at 240 and 340 nm. This instrument is typical of several spectrophotometers offered by various instrument companies. Such instruments are well suited for quantitative measurements where acquisition of an entire spectrum is not often required.

Figure 13-22 shows the optical design of the Cary 100, a more sophisticated, double-beam-in-time recording spectrophotometer. This instrument uses a 30 × 35 mm plane grating having 1200 lines/mm. Its range is from 190 to 900 nm. Bandwidths

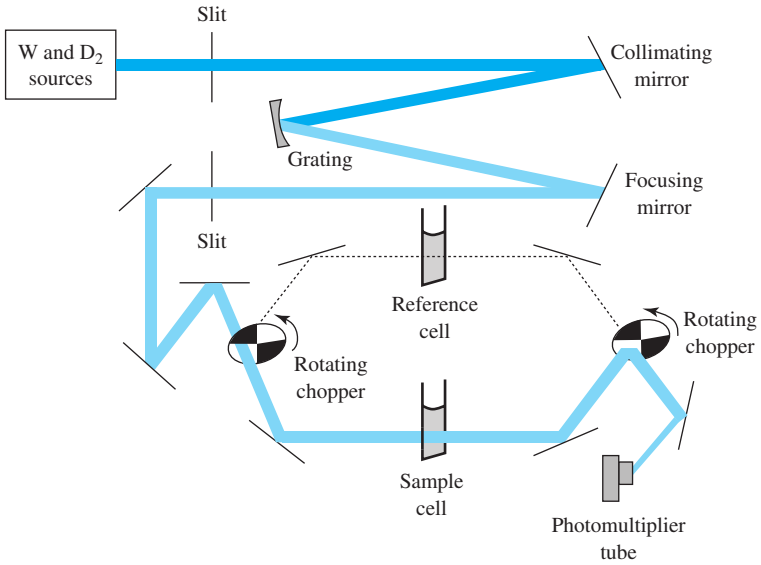

FIGURE 13-22 Schematic of the Cary 100 double-beam spectrophotometer for the UV-visible region. Radiation from one of the sources passes through an entrance slit into the grating monochromator. After exiting the monochromator, the radiation is split into two beams by the chopper. The chopper contains a transparent segment and a mirrored segment in addition to the two dark segments. After passing through the cells, the beams are recombined by the second chopper and strike the photomultiplier tube at different times. The photomultiplier tube sees the following sequence: sample beam, dark, reference beam, dark. (Courtesy of Agilent Technologies, Santa Clara, CA.)

of 0.2 to 4.00 nm can be chosen in 0.1-nm steps by means of a motor-driven slit control system. The instrument has a photometric accuracy of ± 0.00016 *A*; its stray radiation is less than 0.0013% of P_0 at 370 nm and 0.0074% at 220 nm. The absorbance range is from 0 to 3.7 absorbance units. The performance of this instrument is significantly better than that of the double-beam instrument of Figure 13-21; its price is correspondingly higher.

Double-Dispersing Instruments. To enhance spectral resolution and achieve a marked reduction in scattered radiation, a number of instruments have been designed with two gratings serially arranged with an intervening slit; in effect, then, these instruments consist of two monochromators in a series configuration.

The Cary 300 shown in Figure 13-23 uses a premonochromator in front of the same double-beam-in-time instrument shown in Figure 13-22. The second monochromator reduces the stray-light levels to 0.000041% at 370 nm and 0.00008% at 220 nm. This extends the absorbance range to 5.0 absorbance units. Most of the other characteristics are identical to that of the Cary 100. Both units have a double-chopper arrangement that ensures nearly identical light paths for both beams. The two beams strike the photomultiplier tube at essentially the same point, which minimizes errors due to photocathode nonuniformity.

Multichannel Instruments. Array detectors began appearing in UV-visible spectrophotometers in the 1980s. With a diode array, or more recently a CCD array, located at the focal plane of a spectrograph, a spectrum can be obtained by electronic rather than mechanical scanning. All of the data points needed to define a spectrum can thus be gathered essentially simultaneously. The concept of multichannel instruments is attractive because of the potential speed at which spectra can be acquired as well as their applicability to simultaneous multicomponent determinations. By now, several instrument companies offer such instruments as either stand-alone spectrophotometers or as miniature versions.

Figure 13-24 shows a photograph of a miniature fiber-optic spectrometer using a linear CCD array. The optical diagram is similar to that shown in Figure 13-14, except that fiber optics are used to transport the radiation to and from the sample cell. In the version shown, the spectrometer is external to the computer. The output of the array connects to an analog-to-digital converter

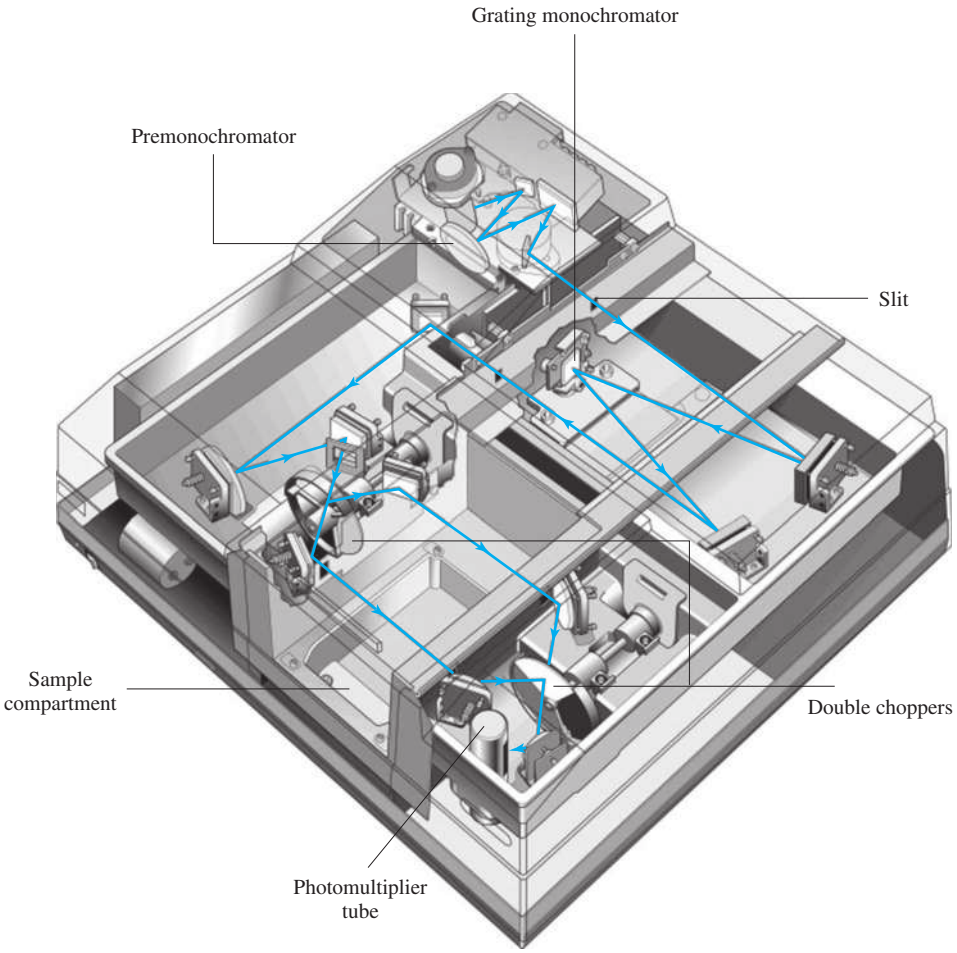

FIGURE 13-23 Optical diagram of the Cary 300 double-dispersing spectrophotometer. The instrument is essentially identical to that shown in Figure 13-22, except that a second monochromator is added immediately after the source. (Agilent Technologies, Santa Clara, CA.)

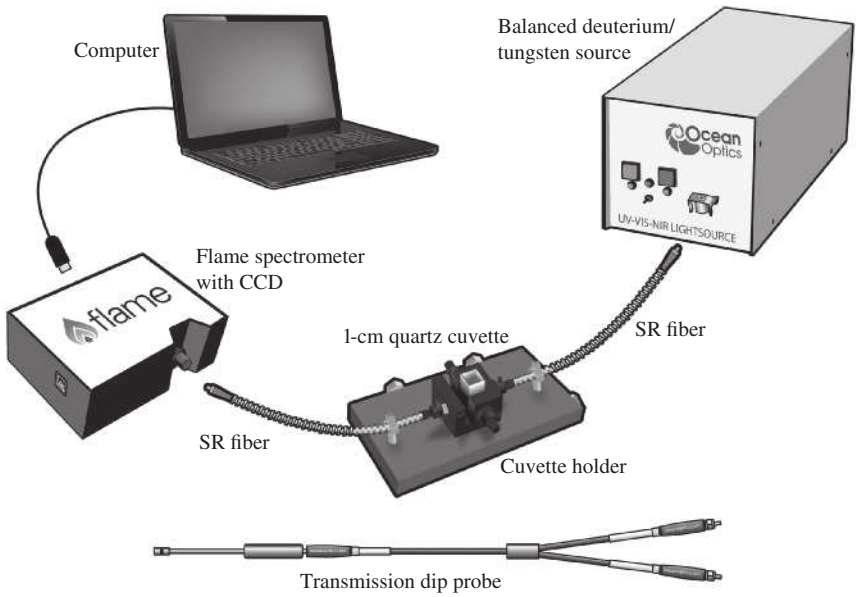

FIGURE 13-24 A multichannel fiber-optic spectrometer. A fiber-optic cable transports the light beam from the source to the sample cell. Another carries the beam from the cuvette to the spectrograph and detector. In some models, the spectrograph and detector are mounted on a circuit board inserted into the computer. A USB port is used to interface to the computer with and its data acquisition system. (Courtesy of Ocean Optics, Inc.)

board in the computer. In other models, the spectrometer contains the converter and interfaces to the computer via a USB port. Such spectrometers are available from about $2000 to more than $5000.

A combined deuterium and tungsten source is shown in Figure 13-24. Separate deuterium and tungsten sources are available for UV only or visible only spectrometers. Some fourteen different gratings are available along with six different entrance slits. No entrance slit is needed with fiber-optic coupling. The spectrometer resolution depends on the grating dispersion and the entrance aperture.

A stand-alone diode-array-based spectrophotometer is illustrated in Figure 13-25. This instrument uses a deuterium source for the UV-visible region (190 to 800 nm) and a tungsten lamp for the visible near-IR region (370 to 1100 nm). A shutter blocks the collimated source radiation or allows it to pass through to the sample cell. A filter can be inserted for stray-light correction. The spectrograph consists of the entrance slit, the grating, and the diode-array detector. A 1024-element photodiode array is used. The nominal bandwidth of the spectrophotometer is 1 nm over the range from 190 to 1100 nm. Stray light is less than 0.05% at 220 nm and less than 0.03% at 340 nm.

With the spectrophotometer of Figure 13-25, scan times can be as short as 0.1 s, but more typically the array is exposed for 1 to 1.5 s. With such short exposure times, photodecomposition of samples is minimized despite the location of the sample between the source and the monochromator. The stability of the source and the electronic system is such that the solvent signal needs to be observed and stored only every 5 to 10 min.

The spectrophotometer shown in Figure 13-25 is designed to interface with most personal computer systems. The exact price of the instrument depends on accessories and options. With a typical setup, the spectrometer sells for less than $20,000.

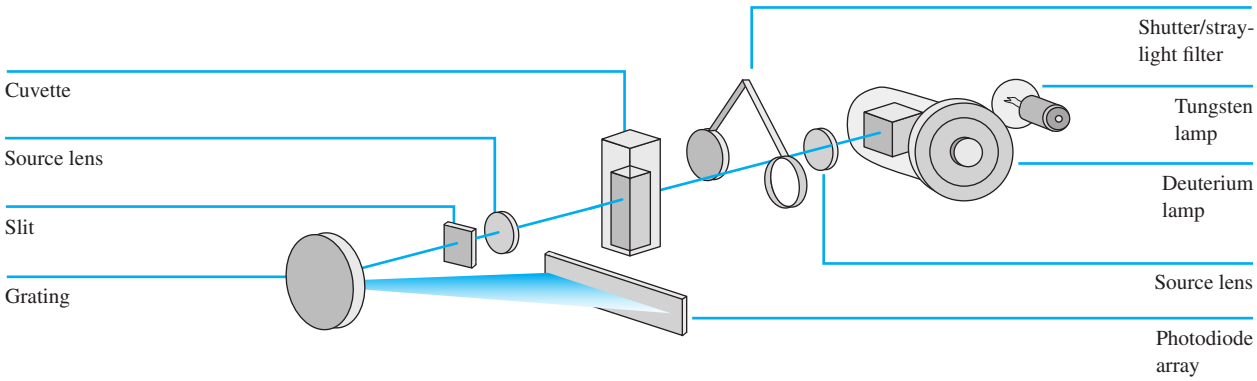

FIGURE 13-25 A multichannel diode-array spectrophotometer, the Agilent Technologies Cary 8454. (Courtesy of Agilent Technologies, Palo Alto, CA.)

» QUESTIONS AND PROBLEMS

*Answers are provided at the end of the book for problems marked with an asterisk.

Problems with this icon are best solved using spreadsheets.

***13-1** Express the following absorbances in terms of percent transmittance:

(a) 0.042 **(d)** 0.379

(b) 0.917 **(e)** 0.435

(c) 0.245 **(f)** 0.513

***13-2** Convert the following transmittance data to absorbances:

(a) 5.38% **(d)** 23.8%

(b) 0.492 **(e)** 0.124

(c) 39.4% **(f)** 15.8%

***13-3** Calculate the percent transmittance of solutions having half the absorbance of the solutions in Problem 13-1.

***13-4** Calculate the absorbance of solutions having twice the percent transmittance of those in Problem 13-2.

***13-5** A solution containing 7.35 ppm $KMnO_4$ had a transmittance of 0.145 in a 1.00-cm cell at 520 nm. Calculate the molar absorptivity of $KMnO_4$ at 520 nm.

13-6 A solution containing 3.92 mg/100 mL of A (335 g/mol) has a transmittance of 64.1% in a 1.50-cm cell at 425 nm. Calculate the molar absorptivity of A at this wavelength.

***13-7** A solution containing the complex formed between Bi(III) and thiourea has a molar absorptivity of 9.32×10^3 L mol^{-1} cm^{-1} at 470 nm.

(a) What is the absorbance of a 4.25×10^{-5} M solution of the complex at 470 nm in a 1.00-cm cell?

(b) What is the percent transmittance of the solution described in (a)?

(c) What is the molar concentration of the complex in a solution that has the absorbance described in (a) when measured at 470 nm in a 2.50-cm cell?

***13-8** At 580 nm, which is the wavelength of its maximum absorption, the complex $Fe(SCN)^{2+}$ has a molar absorptivity of 7.00×10^3 L cm^{-1} mol^{-1}. Calculate

(a) the absorbance of a 4.47×10^{-5} M solution of the complex at 580 nm in a 1.00-cm cell.

(b) the absorbance of a solution in a 2.50-cm cell in which the concentration of the complex is one half that in (a).

(c) the percent transmittance of the solutions described in (a) and (b).

(d) the absorbance of a solution that has half the transmittance of that described in (a).

***13-9** A 2.50-mL aliquot of a solution that contains 6.4 ppm iron(III) is treated with an appropriate excess of KSCN to form the $Fe(SCN)^{2+}$ complex and diluted to 50.0 mL. What is the absorbance of the resulting solution at 580 nm in a 2.50-cm cell? See Problem 13-8 for absorptivity data.

13-10 Zinc(II) and the ligand L form a 1:1 complex that absorbs strongly at 600 nm. As long as the molar concentration of L exceeds that of zinc(II) by a factor of 5, the absorbance depends only on the cation concentration. Neither zinc(II) nor L absorbs at 600 nm. A solution that is 1.59×10^{-4} M in zinc(II) and 1.00×10^{-3} M in L has an absorbance of 0.352 in a 1.00-cm cell at 600 nm. Calculate

(a) the percent transmittance of this solution.

(b) the percent transmittance of this solution in a 2.50-cm cell.

(c) the molar absorptivity of the complex.

QUESTIONS AND PROBLEMS (continued)

13-11 The equilibrium constant for the conjugate acid-base pair

$$HIn + H_2O \rightleftharpoons H_3O^+ + In^-$$

is 8.00×10^{-5}. From the additional information in the following table,

(a) calculate the absorbance at 430 nm and 600 nm for the following indicator concentrations: 3.00×10^{-4} M, 2.00×10^{-4} M, 1.00×10^{-4} M, 0.500×10^{-4} M, and 0.250×10^{-4} M.

(b) plot absorbance as a function of indicator concentration.

Species	Absorption Maximum, nm	Molar Absorptivity	
		430 nm	600 nm
HIn	430	8.04×10^3	1.23×10^3
In^-	600	0.775×10^3	6.96×10^3

13-12 The equilibrium constant for the reaction

$$2CrO_4^{2-} + 2H^+ \rightleftharpoons Cr_2O_7^{2-} + H_2O$$

is 4.2×10^{14}. The molar absorptivities for the two principal species in a solution of $K_2Cr_2O_7$ are

λ	$\varepsilon_1(CrO_4^{2-})$	$\varepsilon_2(Cr_2O_7^{2-})$
345	1.84×10^3	10.7×10^2
370	4.81×10^3	7.28×10^2
400	1.88×10^3	1.89×10^2

Four solutions were prepared by dissolving 4.00×10^{-4}, 3.00×10^{-4}, 2.00×10^{-4}, and 1.00×10^{-4} moles of $K_2Cr_2O_7$ in water and diluting to 1.00 L with a pH 5.60 buffer. Derive theoretical absorbance values (1.00-cm cells) for each solution and plot the data for (a) 345 nm, (b) 370 nm, and (c) 400 nm.

13-13 Describe the differences between the following and list any particular advantages possessed by one over the other.

(a) hydrogen and deuterium discharge lamps as sources for UV radiation.

(b) filters and monochromators as wavelength selectors.

(c) photovoltaic cells and phototubes as detectors for electromagnetic radiation.

(d) photodiodes and photomultiplier tubes.

(e) double-beam-in-space and double-beam-in-time spectrophotometers.

(f) spectrophotometers and photometers.

(g) single-beam and double-beam instruments for absorbance measurements.

(h) conventional and multichannel spectrophotometers.

13-14 A portable photometer with a linear response to radiation registered 56.3 μA with the solvent in the light path. The photometer was set to zero with no light striking the detector. Replacement of the solvent with an absorbing solution yielded a response of 36.7 μA. Calculate

(a) the percent transmittance of the sample solution.

(b) the absorbance of the sample solution.

(c) the transmittance to be expected for a solution in which the concentration of the absorber is one third that of the original sample solution.

(d) the transmittance to be expected for a solution that has twice the concentration of the sample solution.

*13-15 A photometer with a linear response to radiation gave a reading of 529 mV with the solvent in the light path and 272 mV when the solvent was replaced by an absorbing solution. The photometer was set to zero with no light striking the detector. Calculate

(a) the percent transmittance and absorbance of the absorbing solution.

(b) the expected transmittance if the concentration of absorber is one half that of the original solution.

(c) the transmittance to be expected if the light path through the original solution is doubled.

13-16 Why does a deuterium lamp produce a continuum rather than a line spectrum in the UV?

13-17 Why can photomultiplier tubes not be used with IR radiation?

13-18 Why is iodine sometimes introduced into a tungsten lamp?

13-19 Describe the origin of shot noise in a spectrophotometer. How does the relative uncertainty vary with concentration if shot noise is the major noise source?

13-20 Define

(a) dark current.

(b) transducer.

(c) scattered radiation (in a monochromator).

(d) source flicker noise.

(e) cell positioning uncertainty.

(f) beamsplitter.

13-21 Describe how a monochromator, a spectrograph, and a spectrophotometer differ from each other.

13-22 The following data were taken from a diode-array spectrophotometer in an experiment to measure the spectrum of the Co(II)-EDTA complex. The column labeled $P_{solution}$ is the relative signal obtained with sample solution in the cell after subtraction of the dark signal. The column labeled $P_{solvent}$ is the reference signal obtained with only solvent in the cell after subtraction of the dark signal. Find the transmittance at each wavelength, and the absorbance at each wavelength. Plot the spectrum of the compound.

Wavelength, nm	$P_{solvent}$	$P_{solution}$
350	0.002689	0.002560
375	0.006326	0.005995
400	0.016975	0.015143
425	0.035517	0.031648
450	0.062425	0.024978
475	0.095374	0.019073
500	0.140567	0.023275
525	0.188984	0.037448
550	0.263103	0.088537
575	0.318361	0.200872
600	0.394600	0.278072
625	0.477018	0.363525
650	0.564295	0.468281
675	0.655066	0.611062
700	0.739180	0.704126
725	0.813694	0.777466
750	0.885979	0.863224
775	0.945083	0.921446
800	1.000000	0.977237

» QUESTIONS AND PROBLEMS (continued)

13-23 Why do quantitative and qualitative analyses often require different monochromator slit widths?

13-24 The absorbances of solutions containing K_2CrO_4 in 0.05 M KOH were measured in a 1.0-cm cell at 375 nm. The following results were obtained:

Conc. of K_2CrO_4, g/L	*A* at 375 nm
0.0050	0.123
0.0100	0.247
0.0200	0.494
0.0300	0.742
0.0400	0.991

Find the absorptivity of the chromate ion, CrO_4^{2-} in L g^{-1} cm^{-1} and the molar absorptivity of chromate in L mol^{-1} cm^{-1} at 375 nm.

13-25 The absorbances of solutions containing Cr as dichromate $Cr_2O_7^{2-}$ in 1.0 M H_2SO_4 were measured at 440 nm in a 1.0-cm cell. The following results were obtained:

Conc. of Cr, µg/mL	*A* at 440 nm
10.00	0.034
25.00	0.085
50.00	0.168
75.00	0.252
100.00	0.335
200.00	0.669

Find the absorptivity of dichromate (L g^{-1} cm^{-1}) and the molar absorptivity (L mol^{-1} cm^{-1}) at 440 nm.

13-26 A compound X is to be determined by UV-visible spectrophotometry. A calibration curve is constructed from standard solutions of X with the following results: 0.50 ppm, $A = 0.24$; 1.5 ppm, $A = 0.36$; 2.5 ppm, $A = 0.44$; 3.5 ppm, $A = 0.59$; 4.5 ppm, $A = 0.70$. A solution of unknown X concentration had an absorbance of $A = 0.50$. Find the slope and intercept of the calibration curve, the standard error in Y, the concentration of the solution of unknown X concentration, and the standard deviation in the concentration of X. Construct a plot of the calibration curve and determine the unknown concentration by hand from the plot. Compare it to that obtained from the regression line.

Challenge Problem

13-27 The following questions concern the relative concentration uncertainty in spectrophotometry.

(a) If the relative concentration uncertainty is given by Equation 13-13, use calculus to show that the minimum uncertainty occurs at 36.8%*T*. What is the absorbance that minimizes the concentration uncertainty? Assume that s_T is independent of concentration.

(b) Under shot-noise-limited conditions, the relative concentration uncertainty is given by Equation 13-14. Another form of the equation for the shot-noise-limited case is[13]

$$\frac{s_c}{c} = \frac{-kT^{-1/2}}{\ln T}$$

where *k* is a constant. Use calculus and derive the transmittance and absorbance that minimize the concentration uncertainty.

(c) Describe how you could experimentally determine whether a spectrophotometer was operating under Case I, Case II, or Case III conditions.

[13]J. D. Ingle Jr. and S. R. Crouch, *Spectrochemical Analysis*, Upper Saddle River, NJ: Prentice Hall, 1988, Chap. 13.